

# Synthesis and Characterization of OsX{NH=C(Ph)C<sub>6</sub>H<sub>4</sub>}H<sub>2</sub>(P<sup>i</sup>Pr<sub>3</sub>)<sub>2</sub> (X = H, Cl, Br, I): Nature of the H<sub>2</sub> Unit and Its Behavior in Solution

Guada Barea,<sup>†</sup> Miguel A. Esteruelas,<sup>\*,‡</sup> Agustí Lledós,<sup>\*,†</sup> Ana M. López,<sup>‡</sup>  
Enrique Oñate,<sup>‡</sup> and José I. Tolosa<sup>‡</sup>

Departamento de Química Inorgánica, Instituto de Ciencia de Materiales de Aragón,  
Universidad de Zaragoza, CSIC, 50009 Zaragoza, Spain, and Unitat de Química Física,  
Departament de Química, Universitat Autònoma de Barcelona,  
08193 Bellaterra, Barcelona, Spain

Received April 14, 1998

The hexahydride OsH<sub>6</sub>(P<sup>i</sup>Pr<sub>3</sub>)<sub>2</sub> (**1**) reacts with benzophenone imine to give the trihydride derivative OsH<sub>3</sub>{NH=C(Ph)C<sub>6</sub>H<sub>4</sub>}(P<sup>i</sup>Pr<sub>3</sub>)<sub>2</sub> (**2**). The three hydride ligands and the bidentate group of **2** are situated in the equatorial plane of a pentagonal-bipyramidal arrangement of ligands around the metallic center. In solution, two thermally activated exchange processes take place between these hydride ligands, one of them faster than the other one. The reaction of **2** with HCl leads to OsH<sub>3</sub>Cl(NH=CPh<sub>2</sub>)(P<sup>i</sup>Pr<sub>3</sub>)<sub>2</sub> (**3**), which evolves in solution into the elongated dihydrogen compound OsCl{NH=C(Ph)C<sub>6</sub>H<sub>4</sub>}(η<sup>2</sup>-H<sub>2</sub>)(P<sup>i</sup>Pr<sub>3</sub>)<sub>2</sub> (**4**). Complex **4** and the related compounds OsX{NH=C(Ph)C<sub>6</sub>H<sub>4</sub>}(η<sup>2</sup>-H<sub>2</sub>)(P<sup>i</sup>Pr<sub>3</sub>)<sub>2</sub> (X = Br (**5**), I (**6**)) can be also prepared by protonation of **2** with HBF<sub>4</sub>·OEt<sub>2</sub> in dichloromethane and subsequent treatment with NaX (X = Cl, Br, I). The structure of **4** has been determined by X-ray diffraction. The geometry around the osmium atom can be described as a distorted octahedron, with the triisopropylphosphine ligands occupying two relative *trans* positions. The remaining perpendicular plane is formed by the mutually *cis* disposed chloro and dihydrogen ligands and the metalated benzophenone imine group, which has a bite angle of 75.1(1)°. The H<sub>2</sub> unit of **4–6** shows a restricted rotational motion in solution. Thus, the <sup>1</sup>H NMR spectra in the high-field region are a function of the temperature. Lowering the sample temperature leads to a broadening of the dihydrogen resonances. At 213 K, decoalescence occurs, and at 193 K, two signals are clearly observed. Theoretical calculations suggest that the transition states for the hydrogen exchanges in **2** and **4–6** present dihydrogen-like nature.

## Introduction

There are two well-established classes of compounds with more than one hydrogen atom in the coordination sphere of a transition metal: nonclassical dihydrides (or dihydrogens) and classical hydrides.<sup>1</sup>

Dihydrogen compounds contain a hydrogen molecule coordinated to the metal, and the separation between the hydrogen atoms is between 0.8 and 1.0 Å. This range appears suitable to include complexes with a rapidly spinning dihydrogen unit whose properties are perturbed little from those of free dihydrogen gas. Thus, the molecular hydrogen, when coordinated, exhibits

several distinct spectroscopic features: for example low *T*<sub>1</sub>(min) and high *J*(HD) constants for the M(HD) isotopomer. These have helped to characterize the complexes, to estimate the hydrogen–hydrogen distance, and hence, to get information on the amount of stretching of the hydrogen–hydrogen bond.<sup>1f,2</sup>

Hydrides have the hydrogen–hydrogen distances expected for two ligands occupying the usual stereochemical positions in coordination polyhedra (>1.6 Å). Such distances usually result in little communication between the nuclei: a long *T*<sub>1</sub>(min) (>90 ms at 200 MHz) and very small *J*(HD) constant for the M(H)(D)

<sup>†</sup> Universitat Autònoma de Barcelona.

<sup>‡</sup> Universidad de Zaragoza.

(1) (a) Kubas, G. *J. Acc. Chem. Res.* **1988**, *21*, 120. (b) Kubas, G. *J. Comments Inorg. Chem.* **1988**, *7*, 17. (c) Henerson, R. H. *Transition Met. Chem.* **1988**, *13*, 474. (d) Crabtree, R. H.; Hamilton, D. G. *Adv. Organomet. Chem.* **1988**, *28*, 299. (e) Crabtree, R. H. *Acc. Chem. Res.* **1990**, *23*, 95. (f) Jessop, P. G.; Morris, R. H. *Coord. Chem. Rev.* **1992**, *121*, 155. (g) Crabtree, R. H. *Angew. Chem., Int. Ed. Engl.* **1993**, *32*, 789. (h) Heinekey, D. M.; Oldham, J. *Chem. Rev.* **1993**, *93*, 913. (i) Morris, R. H. *Can. J. Chem.* **1996**, *74*, 1907.

(2) (a) Hamilton, D. G.; Crabtree, R. H. *J. Am. Chem. Soc.* **1988**, *110*, 4126. (b) Earl, K. A.; Jia, G.; Maltby, P. A.; Morris, R. H. *J. Am. Chem. Soc.* **1991**, *113*, 3027. (c) Bautista, M. T.; Capellani, E. P.; Drouin, S. D.; Morris, R. H.; Schweitzer, C. T.; Sella, A.; Zubkowski, J. P. *J. Am. Chem. Soc.* **1991**, *113*, 4876. (d) Desrosiers, P. J.; Cai, P.; Lin, Z.; Richards, R.; Halpern, J. *J. Am. Chem. Soc.* **1991**, *113*, 4173. (e) Heinekey, D. M.; Luther, T. A. *Inorg. Chem.* **1996**, *35*, 4396. (f) Maltby, P. A.; Schlaf, M.; Steinbeck, M.; Lough, A. J.; Morris, R. H.; Klooster, W. T.; Koetzle, T. F.; Srivastava, R. C. *J. Am. Chem. Soc.* **1996**, *118*, 5396. (g) Hush, N. S. *J. Am. Chem. Soc.* **1997**, *119*, 1717. (h) Luther, T. A.; Heinekey, D. M. *J. Am. Chem. Soc.* **1997**, *119*, 6688.

isotopomer.<sup>1,3</sup> Variable-temperature <sup>1</sup>H NMR spectra of some of these compounds have revealed dynamic behaviors associated with thermally activated exchange processes, involving the hydride positions. Theoretical studies on the hydride exchange processes in the trihydrides [CpIrH<sub>3</sub>L]<sup>+</sup> (L = PH<sub>3</sub>, CO),<sup>4</sup> OsH<sub>3</sub>(η<sup>2</sup>-H<sub>2</sub>BH<sub>2</sub>)-(PH<sub>3</sub>)<sub>2</sub>,<sup>5</sup> and [CpMH<sub>3</sub>]<sup>n+</sup> (M = Mo, W, n = 1; M = Nb, Ta, n = 0)<sup>6</sup> suggest that the exchange takes place through a transition state, which is reached by a shortening of the hydrogen–hydrogen distance and a lengthening of the M–H distance, and from a geometrical point of view, the exchange presents a η<sup>2</sup>-H<sub>2</sub> complex-like nature.

In addition to these two types of compounds, there is a group of complexes that is difficult to classify, with hydrogen–hydrogen distances between 1.0 and 1.5 Å. These compounds are seen as frozen structures at various points on the reaction profile path for the oxidative addition–reductive elimination of molecular hydrogen at the metallic center. Thus, it is assumed that the potential energy versus the hydrogen–hydrogen distance plot for such a complex has a minimum at the equilibrium hydrogen–hydrogen distance.<sup>1f</sup> An indicator of a complex containing a ligand of this type (elongated dihydrogen, also referred as to “stretched”) is the *J*(HD) value in the M(HD) isotopomer. It has been proposed that when this coupling falls between 5 and 25 Hz, such a form of the ligand is present.<sup>7</sup>

The spectroscopic properties of an elongated dihydrogen complex might also be explained by the averaging of the properties of a dihydride compound and a complex with a rotating dihydrogen ligand, caused by a low-energy bond-splitting/bond-forming process. In such a case, a potential surface with a double well must be found.<sup>1f</sup>

Rotational motion of the elongated dihydrogen structure is assumed to be restricted. However, only very recently has this been proven. In 1995, Jalón, Otero, Chaudret, and co-workers<sup>8</sup> reported the preparation of the complex [Nb(η<sup>5</sup>-C<sub>5</sub>Me<sub>5</sub>)<sub>2</sub>(η<sup>2</sup>-H<sub>2</sub>)(PMe<sub>2</sub>Ph)]CF<sub>3</sub>CO<sub>2</sub> (*J*(HD) = 15 Hz) by protonation at low temperature of the corresponding neutral hydridoniobium complex. One

of the interesting points of this dihydrogen complex lies in the fact that the activation barrier for the rotation of the dihydrogen ligand is relatively high (ca. 10 kcal mol<sup>-1</sup>). As a consequence of this, the rotation of the HD molecule in the isotopomer [Nb(η<sup>5</sup>-C<sub>5</sub>Me<sub>5</sub>)<sub>2</sub>(η<sup>2</sup>-HD)(PMe<sub>2</sub>-Ph)]CF<sub>3</sub>CO<sub>2</sub> is blocked on the NMR time scale. In the high-field region of the <sup>1</sup>H NMR spectrum of [Nb(η<sup>5</sup>-C<sub>5</sub>-Me<sub>5</sub>)<sub>2</sub>(η<sup>2</sup>-H<sub>2</sub>)(PMe<sub>2</sub>Ph)]CF<sub>3</sub>CO<sub>2</sub>, a single resonance is observed for the two hydrogen atoms at high temperatures. When the temperature is lowered, decoalescence is not observed. However, a slowly rotating HD unit in the isotopomer [Nb(η<sup>5</sup>-C<sub>5</sub>Me<sub>5</sub>)<sub>2</sub>(η<sup>2</sup>-HD)(PMe<sub>2</sub>Ph)]CF<sub>3</sub>CO<sub>2</sub> enables the observation of two interconverting rotamers. Subsequently, a similar phenomenon was observed for [Ta(η<sup>5</sup>-C<sub>5</sub>H<sub>5</sub>)<sub>2</sub>(η<sup>2</sup>-HD)(CO)]BF<sub>4</sub> (*J*(HD) = 27.5 Hz)<sup>9</sup> and [Nb(η<sup>5</sup>-C<sub>5</sub>H<sub>4</sub>SiMe<sub>3</sub>)<sub>2</sub>(η<sup>2</sup>-H<sub>2</sub>)(CNR)]<sup>+</sup> (*J*(HD) = 30 Hz).<sup>10</sup>

As a part of the work of our groups on osmium polyhydride chemistry,<sup>3c,5,11</sup> in this paper we report the synthesis and characterization of complexes of formula OsX{NH=C(Ph)C<sub>6</sub>H<sub>4</sub>}H<sub>2</sub>(P<sup>i</sup>Pr<sub>3</sub>)<sub>2</sub> (X = H, Cl, Br, I), a theoretical study on OsH<sub>2</sub> interactions in these systems, and the behavior of the H<sub>2</sub> unit in solution.

## Results and Discussion

**1. OsH<sub>3</sub>{NH=C(Ph)C<sub>6</sub>H<sub>4</sub>}H<sub>2</sub>(P<sup>i</sup>Pr<sub>3</sub>)<sub>2</sub>.** Recently, we have reported that the hexahydride compound OsH<sub>6</sub>(P<sup>i</sup>Pr<sub>3</sub>)<sub>2</sub> (**1**) reacts with tetrafluorobenzobarrelene, 2,5-norbornadiene, and 1,3-cyclohexadiene to afford the dihydride diolefin derivatives OsH<sub>2</sub>(η<sup>4</sup>-TFB)(P<sup>i</sup>Pr<sub>3</sub>)<sub>2</sub>, OsH<sub>2</sub>(η<sup>4</sup>-NBD)(P<sup>i</sup>Pr<sub>3</sub>)<sub>2</sub>, and OsH<sub>2</sub>(η<sup>4</sup>-cyclohexadiene)(P<sup>i</sup>Pr<sub>3</sub>)<sub>2</sub>, respectively. The protonation of OsH<sub>2</sub>(η<sup>4</sup>-TFB)(P<sup>i</sup>Pr<sub>3</sub>)<sub>2</sub> and OsH<sub>2</sub>(η<sup>4</sup>-NBD)(P<sup>i</sup>Pr<sub>3</sub>)<sub>2</sub> leads to the trihydride diolefin cations [OsH<sub>3</sub>(η<sup>4</sup>-TFB)(P<sup>i</sup>Pr<sub>3</sub>)<sub>2</sub>]<sup>+</sup> and [OsH<sub>3</sub>(η<sup>4</sup>-NBD)(P<sup>i</sup>Pr<sub>3</sub>)<sub>2</sub>]<sup>+</sup>, while under the same conditions, the complex OsH<sub>2</sub>(η<sup>4</sup>-cyclohexadiene)(P<sup>i</sup>Pr<sub>3</sub>)<sub>2</sub> yields the dihydride cyclohexenyl derivative [OsH<sub>2</sub>(η<sup>3</sup>-C<sub>6</sub>H<sub>9</sub>)(P<sup>i</sup>Pr<sub>3</sub>)<sub>2</sub>]<sup>+</sup>, which shows an agostic interaction between the osmium center and one of the two *endo*-CH bonds adjacent to the π-allyl unit.<sup>3c</sup>

Previously, we had observed that complex **1** reacts with 2,2'-biimidazole to give the trihydride compound OsH<sub>3</sub>(Hbiim)(P<sup>i</sup>Pr<sub>3</sub>)<sub>2</sub>, which affords the heterobimetallic complexes (P<sup>i</sup>Pr<sub>3</sub>)<sub>2</sub>H<sub>3</sub>Os(μ-biim)M(COD) by reaction with the dimers [M(μ-OME)(COD)]<sub>2</sub> (M = Rh, Ir).<sup>11c</sup>

Continuing with the study of the reactivity of **1**, we have now carried out the reaction of this complex with benzophenone imine. Treatment under reflux of a toluene solution of **1** with ca. 1 equiv of benzophenone imine leads after 6 h to a red solution, from which the trihydride complex OsH<sub>3</sub>{NH=C(Ph)C<sub>6</sub>H<sub>4</sub>}H<sub>2</sub>(P<sup>i</sup>Pr<sub>3</sub>)<sub>2</sub> was isolated as a red solid in 80% yield (eq 1).

(9) Sabo-Etienne, S.; Chaudret, B.; Abou el Makarim, H. A.; Barthelat, J.-C.; Daudey, J.-P.; Ulrich, S.; Limbach, H.-H.; Moise, C. *J. Am. Chem. Soc.* **1995**, *117*, 11602.

(10) Antiñolo, A.; Carrillo-Hermosilla, F.; Fajardo, M.; García-Yuste, S.; Otero, A.; Camanyes, S.; Maseras, F.; Moreno, M.; Lledós, A.; Lluch, J. M. *J. Am. Chem. Soc.* **1997**, *119*, 6107.

(11) (a) Esteruelas, M. A.; Jean, Y.; Lledós, A.; Oro, L. A.; Ruiz, N.; Volatron, F. *Inorg. Chem.* **1994**, *33*, 3609. (b) Buil, M. L.; Espinet, P.; Esteruelas, M. A.; Lahoz, F. J.; Lledós, A.; Martínez-Illarduya, J. M.; Maseras, F.; Modrego, J.; Oñate, E.; Oro, L. A.; Sola, E.; Valero, C. *Inorg. Chem.* **1996**, *35*, 1250. (c) Esteruelas, M. A.; Lahoz, F. J.; López, A. M.; Oñate, E.; Oro, L. A.; Ruiz, N.; Sola, E.; Tolosa, J. I. *Inorg. Chem.* **1996**, *35*, 7811.

(3) (a) Bakmutov, V. I.; Vorontsov, E. V.; Vymenits, A. B. *Inorg. Chem.* **1995**, *34*, 214. (b) Gusev, D. G.; Kuhlman, R. L.; Renkema, K. B.; Eisenstein, O.; Caulton, K. G. *Inorg. Chem.* **1996**, *35*, 6775. (c) Castillo, A.; Esteruelas, M. A.; Oñate, E.; Ruiz, N. *J. Am. Chem. Soc.* **1997**, *119*, 9691.

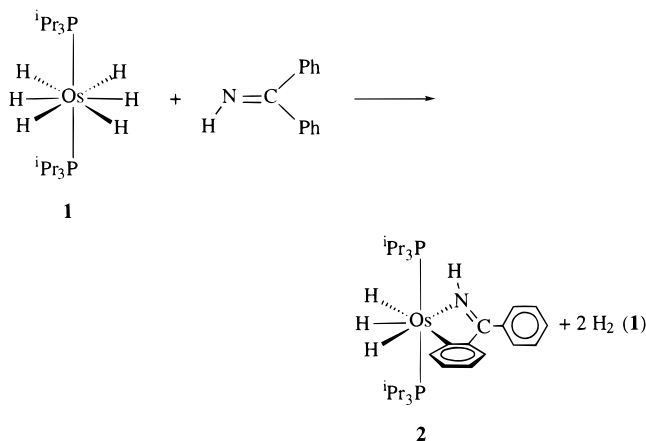
(4) Jarid, A.; Moreno, M.; Lledós, A.; Lluch, J. M.; Bertrán, J. *J. Am. Chem. Soc.* **1995**, *117*, 1069.

(5) Demachy, I.; Esteruelas, M. A.; Jean, Y.; Lledós, A.; Maseras, F.; Oro, L. A.; Valero, C.; Volatron, F. *J. Am. Chem. Soc.* **1996**, *118*, 8388.

(6) Camanges, S.; Maseras, F.; Moreno, M.; Lledós, A.; Lluch, J. M.; Bertran, J. *J. Am. Chem. Soc.* **1996**, *118*, 4617.

(7) (a) Chinn, M. S.; Heinekey, D. M. *J. Am. Chem. Soc.* **1990**, *112*, 5166. (b) Collman, J. P.; Wagenknecht, P. S.; Hembre, R. T.; Lewis, N. S. *J. Am. Chem. Soc.* **1990**, *112*, 1294. (c) Michos, D.; Luo, X.-L.; Howard, J. A. K.; Crabtree, R. H. *Inorg. Chem.* **1992**, *31*, 3914. (d) Albinati, A.; Bakmutov, V. I.; Caulton, K. G.; Clot, E.; Eckert, J.; Eisenstein, O.; Gusev, D. G.; Grushim, V. V.; Hauger, B. E.; Klooster, W. T.; Koetzle, T. F.; McMullan, R. K.; O'Loughlin, T. J.; Pélissier, M.; Ricci, J. S.; Sigalas, M. P.; Vymenits, A. B. *J. Am. Chem. Soc.* **1993**, *115*, 7300. (e) Hasegawa, T.; Li, Z.; Parkin, S.; Hope, H.; McMullan, R. K.; Koetzle, T. F.; Taube, H. *J. Am. Chem. Soc.* **1994**, *116*, 4352. (f) Li, Z.-W.; Taube, H. *J. Am. Chem. Soc.* **1994**, *116*, 9506. (g) Schlaf, M.; Lough, A. J.; Maltby, P. A.; Morris, R. H. *Organometallics* **1996**, *15*, 2270. (h) Chin, R. Y.; Barrera, J.; Dubois, R. H.; Helberg, L. E.; Sabat, M.; Bartucz, T. Y.; Lough, A. J.; Morris, R. H.; Harman, W. D. *Inorg. Chem.* **1997**, *36*, 3553. (i) Gelabert, R.; Moreno, M.; Lluch, J. M.; Lledós, A. *J. Am. Chem. Soc.* **1997**, *119*, 9840.

(8) Jalón, F. A.; Otero, A.; Manzano, B. R.; Villaseñor, E.; Chaudret, B. *J. Am. Chem. Soc.* **1995**, *117*, 10123.



The spectroscopic data for **2** agree well with the structure proposed in eq 1. The IR spectrum in Nujol shows the  $\nu(\text{NH})$  vibration at  $3348\text{ cm}^{-1}$  along with three bands at  $2143$ ,  $2106$ , and  $1942\text{ cm}^{-1}$ , corresponding to the  $\nu(\text{Os}-\text{H})$  vibrations. In the region  $\delta$  195–175 the  $^{13}\text{C}\{^1\text{H}\}$  NMR spectrum contains two triplets at  $194.6$  ( $J(\text{PC}) = 5.6\text{ Hz}$ ) and  $179.9$  ( $J(\text{PC}) = 3.0\text{ Hz}$ ) ppm. The triplet at  $179.9$  ppm was assigned to the carbon atom of the  $\text{C}=\text{N}$  group by comparison of this spectrum with those previously reported for the complexes  $\text{Os}(\text{C}_2\text{Ph})\{\text{NH}=\text{C}(\text{Ph})\text{C}_6\text{H}_4\}(\text{CO})(\text{P}^i\text{Pr}_3)_2$  ( $\delta$  185.7;  $J(\text{PC}) = 2.9\text{ Hz}$ ),<sup>12</sup>  $[\text{Ru}\{\text{N}(\text{Ph})=\text{C}(\text{R})\text{C}_6\text{H}_4\}(\eta^6\text{-C}_6\text{Me}_6)(\text{PMe}_3)]\text{BF}_4$  ( $\text{R} = \text{H}$  ( $\delta$  175.3),  $\text{R} = \text{CH}_3$  ( $\delta$  180.4)),<sup>13</sup>  $[\text{Os}\{\text{NH}=\text{C}(\text{Ph})\text{C}_6\text{H}_4\}(\eta^6\text{-C}_6\text{H}_3\text{Me}_3)(\text{P}^i\text{Pr}_3)]\text{PF}_6$  ( $\delta$  191.72,  $J(\text{PC}) = 1.5\text{ Hz}$ ),<sup>14</sup>  $\text{Ru}(\eta^5\text{-C}_5\text{H}_5)\{\text{NH}=\text{C}(\text{Ph})\text{C}_6\text{H}_4\}(\text{PPh}_3)$  ( $\delta$  183.24,  $J(\text{PC}) = 2.0\text{ Hz}$ )<sup>15</sup> and  $\text{OsH}\{\text{NH}=\text{C}(\text{Ph})\text{C}_6\text{H}_4\}(\text{CO})(\text{P}^i\text{Pr}_3)_2$  ( $\delta$  181.2),<sup>16</sup> while the triplet at  $194.6$  ppm was assigned to the aromatic carbon bonded to the osmium. In agreement with the mutually *trans* disposition of the phosphine ligands, the  $^{31}\text{P}\{^1\text{H}\}$  NMR spectrum in toluene- $d_8$  shows a singlet at  $26.8$  ppm, which is temperature-invariant between  $353$  and  $193\text{ K}$ . At room temperature the  $^1\text{H}$  NMR spectrum in toluene- $d_8$  exhibits an NH resonance at  $10.25$  ppm, along with the expected resonances for the protons of the metalated and nonmetalated phenyl rings, and the typical resonances for the triisopropylphosphine protons. Furthermore, in the high-field region, the spectrum contains two broad resonances at  $-9.07$  (2H) and  $-9.87$  (1H) ppm.

In contrast to the  $^{31}\text{P}\{^1\text{H}\}$  NMR spectrum, the  $^1\text{H}$  NMR spectrum is temperature-dependent. At  $353\text{ K}$ , the spectrum shows in the hydride region a single triplet resonance at  $-9.39$  ppm with a P–H coupling constant of  $15.4\text{ Hz}$ . This observation is consistent with the operation of two thermally activated site exchange processes, which proceed at rates sufficient to lead to a

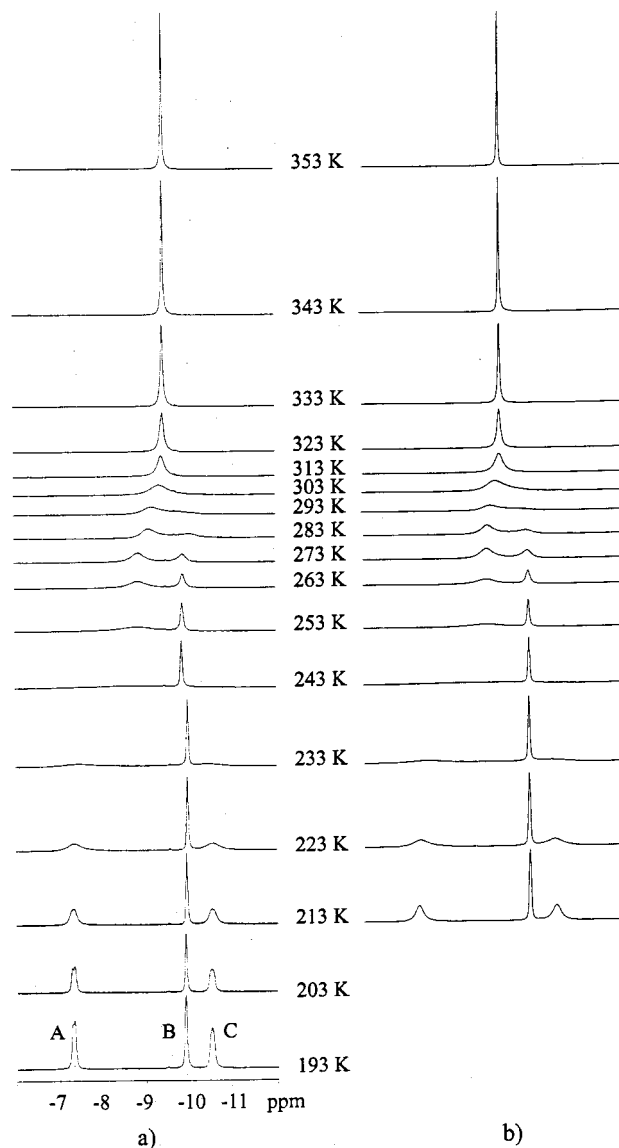


**Figure 1.**  $^1\text{H}\{^{31}\text{P}\}$  NMR spectra (300 MHz, toluene- $d_8$ ) in the high-field region of  $[\text{OsH}_3\{\text{NH}=\text{C}(\text{Ph})\text{C}_6\text{H}_4\}(\text{P}^i\text{Pr}_3)_2]$  (**2**): (a) observed; (b) simulated.

single hydride resonance. Consistent with this, lowering the sample temperature leads to broadening of the resonance. At  $283\text{ K}$ , the first decoalescence occurs, and at  $223\text{ K}$ , the second one takes place. At this temperature, an  $\text{ABCX}_2$  spin system ( $\text{X} = ^{31}\text{P}$ ) is observed, which becomes well-resolved at  $193\text{ K}$ . The  $^1\text{H}\{^{31}\text{P}\}$  spectra (Figure 1) are simplified to the expected ABC spin system. The values of the chemical shifts of the A ( $\delta$   $-7.3$ ), B ( $\delta$   $-9.9$ ), and C ( $\delta$   $-10.5$ ) sites as well as the values of H–H coupling constants ( $J(\text{AB}) = 0.0\text{ Hz}$ ,  $J(\text{AC}) = 15.0\text{ Hz}$ ,  $J(\text{BC}) = 13.5\text{ Hz}$ ) show no significant temperature dependence. This is in contrast with that observed for the related trihydride complexes  $\text{OsH}_3(\text{Hbiim})(\text{P}^i\text{Pr}_3)_2$  ( $\text{Hbiim} = 2,2'$ -biimidazole)<sup>11c</sup> and  $[\text{OsH}_3(\eta^4\text{-diolefin})(\text{P}^i\text{Pr}_3)_2]\text{BF}_4$  (diolefin = 2,5-norbornadiene, tetrafluorobenzobarrelene),<sup>3c</sup> where the H–H coupling constants are very sensitive to temperature, as a result of a quantum-mechanical exchange process.

To assign the hydride resonances to the hydride ligands of **2**, we have carried out a NOESY experiment, at  $193\text{ K}$ . As a result of this experiment (Figure 2), we

(12) Esteruelas, M. A.; Lahoz, F. J.; López, A. M.; Oñate, E.; Oro, L. A. *Organometallics* **1995**, *14*, 2496.

(13) Martin, G. C.; Boncella, J. M. *Organometallics* **1989**, *8*, 2968.

(14) Daniel, T.; Müller, M.; Werner, H. *Inorg. Chem.* **1991**, *30*, 3118.

(15) Werner, H.; Daniel, T.; Knaup, W.; Nürnberg, O. *J. Organomet. Chem.* **1993**, *362*, 309.

(16) (a) Daniel, T.; Werner, H. *Z. Naturforsch., B* **1992**, *4*, 1707. (b) Albéniz, M. J.; Buil, M.; Esteruelas, M. A.; López, A. M. *J. Organomet. Chem.* **1997**, *545–546*, 495.

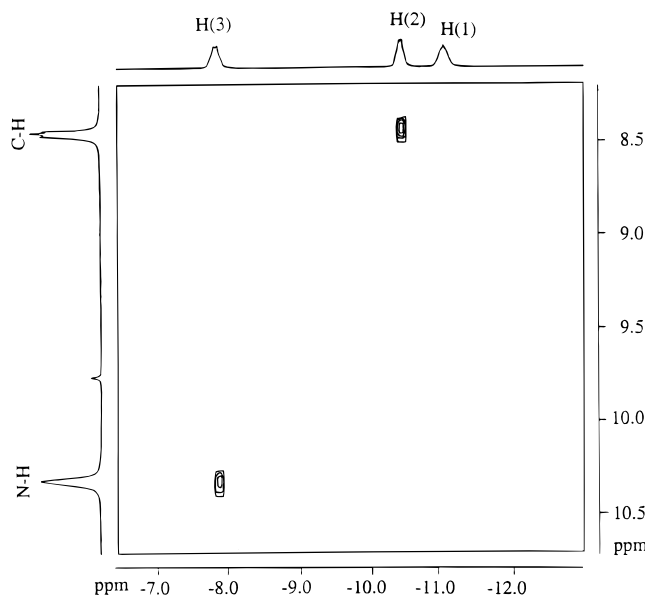


**Figure 2.** Partial view of the  $^1\text{H}$  NOESY NMR spectrum (300 MHz, dichloromethane- $d_2$ ) of  $\text{OsH}_3\{\text{NH}=\text{C}(\text{Ph})\text{C}_6\text{H}_4\}(\text{P}^i\text{Pr}_3)_2$  (**2**) at 193 K.

assigned the resonance C to the central hydride ligand (H(1)), the resonance B to the hydride ligand disposed *trans* to the nitrogen atom (H(2)), and the resonance A to the hydrido ligand disposed *trans* to the ortho-metalated phenyl ring (H(3)).

$T_1$  values of the hydrogen nuclei of the  $\text{OsH}_3$  unit were determined in toluene- $d_8$  as solvent over the temperature range 283–198 K. The  $T_1$ (min) values of the three hydrides H(3) (89 ms), H(2) (114 ms), and H(1) (90 ms) occur at the same temperature (223 K). These values are in agreement with those previously found for the hydride ligands of the complexes  $\text{OsH}_3(\text{Hbiim})(\text{P}^i\text{Pr}_3)_2$  (77 and 86 ms)<sup>11c</sup> and  $[\text{OsH}_3(\eta^4\text{-diolefin})(\text{P}^i\text{Pr}_3)_2]\text{BF}_4$  (diolefin = TFB (69 and 118 ms), NBD (64 ms and 85 ms))<sup>3c</sup> and support the trihydride character of **2**.

To obtain a more complete structural description of complex **2**, we have also performed theoretical calculations on the model system  $\text{OsH}_3\{\text{NH}=\text{C}(\text{H})\text{C}_6\text{H}_4\}(\text{PH}_3)_2$  (**2t**). The geometry of **2t** has been fully optimized at the B3LYP level. The main geometrical parameters are collected in the first column of Table 1, and the structure is depicted in Figure 3.

The characterization of **2t** as a trihydride species is confirmed, with H–H distances of 1.72 Å. The complex presents a quite regular pentagonal-bipyramidal geometry, with the three hydride ligands and the bidentate group in the equatorial plane. Bond angles between the equatorial ligands are very close to the ideal value of 72°. The metal–hydride bond distances for the central hydride (H(1); 1.635 Å) and the terminal hydride *trans* to the N atom (H(2); 1.633 Å) are practically the same, while the separation Os–H(3) (*trans* to C) is appreciably longer (1.671 Å). This fact suggests a weaker M–H(3) bond and thus a lesser electron donation in this site. To verify that the three hydrides are different from an electronic point of view, we have computed the atomic charges for the three hydrogen atoms, by integration of

**Table 1.** Selected Geometrical Parameters (Å and deg) of the B3LYP Optimized Structures of the  $\text{OsH}_2\text{X}\{\text{NH}=\text{C}(\text{H})\text{C}_6\text{H}_4\}(\text{PH}_3)_2$  (X = H (**2t**)) and  $\text{OsX}\{\text{NH}=\text{C}(\text{H})\text{C}_6\text{H}_4\}(\eta^2\text{-H}_2)(\text{PH}_3)_2$  (X = Cl (**4t**), Br (**5t**), I (**6t**)) Systems

	2t (X = H)	4t (X = Cl)	5t (X = Br)	6t (X = I)
Os–H(1)	1.635	1.633	1.632	1.632
Os–H(2)	1.633	1.607	1.610	1.611
Os–X	1.671	2.534	2.688	2.873
Os–N	2.146	2.126	2.129	2.134
Os–P	2.320	2.334	2.340	2.341
N–H <sub>n</sub>	1.015	1.023	1.019	1.019
H(1)–H(2)	1.723	1.483	1.475	1.465
H(1)–X	1.722	2.695	2.783	2.894
X···H <sub>n</sub>	2.532	2.737	2.841	3.020
H(1)–Os–X	62.8	77.3	75.8	74.3
H(1)–Os–H(2)	63.6	54.5	54.2	53.7
H(1)–Os–N	142.8	157.3	156.8	156.8
H(1)–Os–C(3)	142.0	126.8	127.2	127.2
X–Os–H(2)	126.4	131.8	130.1	128.0
X–Os–N	80.0	80.0	81.0	82.5
X–Os–C(3)	159.2	155.9	156.9	158.5
H(2)–Os–N	153.6	148.2	148.9	149.5
H(2)–Os–C(3)	78.4	72.3	73.0	73.5
N–Os–C(3)	75.2	75.9	75.9	76.0
N–Os–P	93.6	92.8	92.8	92.9
C(3)–Os–P	91.6	92.5	92.5	92.5
P–Os–P	172.6	173.3	173.3	173.2
Os–N–H <sub>n</sub>	122.8	121.3	120.1	121.1

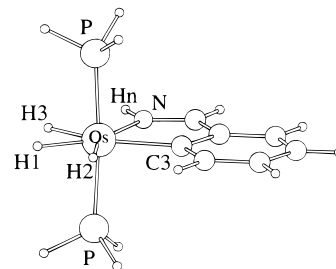


**Figure 3.** Optimized structure of  $\text{OsH}_3\{\text{NH}=\text{C}(\text{Ph})\text{C}_6\text{H}_4\}(\text{PH}_3)_2$  (**2t**).

the charge density over the atomic domain.<sup>17</sup> In agreement with the hydride nature of **2t**, the Bader net charges are negative, similar to those obtained with the same methodology in the Os(IV) complex  $\text{OsH}_4(\text{PH}_3)_3$ .<sup>18</sup> However, the charge that each hydride bears is detectably different:  $-0.19e$  for H(1),  $-0.24e$  for H(2), and  $-0.29e$  for H(3). Therefore, it seems to be clear that in the site *trans* to the C atom less electronic density is transferred from the ligand to the metal.

The spectra shown in Figure 1 indicate that, between the hydride ligands of **2**, two thermally activated site exchange processes take place. One of them is faster than the other one. The slower exchange process involves the hydride ligand disposed *trans* to the nitrogen atom (H(2)) and the central hydrido ligand (H(1)), while the faster exchange process takes place between H(1) and the hydride ligand located *trans* to the ortho-metalated phenyl ring (H(3)).

Line shape analysis of the spectra shown in Figure 1 allows the calculation of the rate constants for both

(17) (a) Bader, R. F. W.; Nguyen-Dang, T. T. *Adv. Quantum Chem.* **1981**, *14*, 63. (b) Biegler-König, F. W.; Bader, R. F. W.; Tang, T. H. *J. Comput. Chem.* **1982**, *3*, 317.

(18) Maseras, F.; Lledós, A.; Costas, M.; Poblet, J. M. *Organometallics* **1996**, *15*, 2947.

**Table 2. Rate Constants (s<sup>-1</sup>) for the Intramolecular Site-Exchange Processes in**



T (K)	k[H(1)–H(3)]	k[H(1)–H(2)]	T (K)	k[H(1)–H(3)]	k[H(1)–H(2)]
213	160		293	69 000	650
223	385		303	120 000	1 100
233	980		313	200 000	3 000
243	2 400		323	300 000	9 000
253	5 500	15	333	480 000	28 000
263	10 500	70	343	760 000	85 000
273	20 500	210	353	1 100 000	260 000
283	39 000	350			

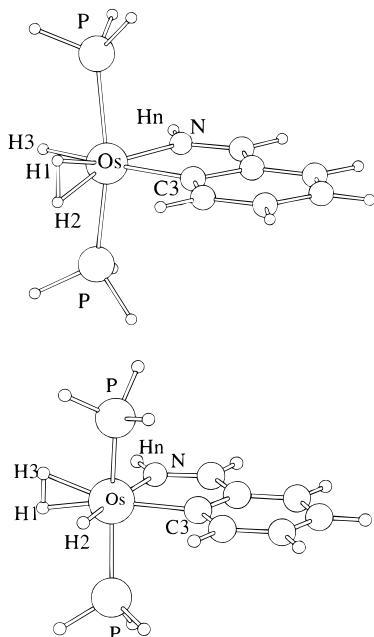


**Figure 4.** Transition-state structures for the hydrogen exchange processes in **2t**: (top) **2t-TStN**; (bottom) **2t-TStC**.

thermal exchange processes at different temperatures (Table 2). The activation parameters obtained from the Eyring analysis are  $\Delta H^\ddagger = 18.2(\pm 0.7)$  kcal mol<sup>-1</sup> and  $\Delta S^\ddagger = 17(\pm 2)$  cal K<sup>-1</sup> mol<sup>-1</sup> for the H(1)–H(2) exchange and  $\Delta H^\ddagger = 8.9(\pm 0.2)$  kcal mol<sup>-1</sup> and  $\Delta S^\ddagger = -5.8(\pm 0.6)$  cal K<sup>-1</sup> mol<sup>-1</sup> for the H(1)–H(3) exchange.

To find the transition states of these processes and the mechanism of the exchanges, theoretical calculations were carried out. The transition states (**2t-TStN** for the H(1)–H(2) exchange and **2t-TStC** for the H(1)–H(3) exchange) were calculated by a complete optimization of the geometry of **2t** with H(1) and H(2) (**2t-TStN**) and H(1) and H(3) (**2t-TStC**) twisted 90° with respect to the position in the minimum. The structures found in this way are shown in Figure 4. Selected bond distances and angles are collected in Table 3.

Both transition states can be described as octahedral osmium(II) species containing dihydrogen ligands. The Os( $\eta^2$ -H<sub>2</sub>) nature is supported by the hydrogen–hydrogen distances between the exchanging atoms, 0.906 Å in **2t-TStN** and 0.896 Å in **2t-TStC**. This agrees well with the mechanism initially proposed by Limbach et al.<sup>19</sup> for the hydrogen exchange in trihydride complexes and theoretically corroborated for the OsH<sub>3</sub>( $\eta^2$ -H<sub>2</sub>BH<sub>2</sub>)-(PR<sub>3</sub>)<sub>2</sub> system<sup>5</sup> and iridium trihydride<sup>4</sup> and metallocene trihydride complexes.<sup>6</sup>

(19) Limbach, H. H.; Scherer, G.; Maurer, M.; Chaudret, B. *Angew. Chem., Int. Ed. Engl.* **1992**, *31*, 1369.

**Table 3. Selected Geometrical Parameters (Å and deg) of the B3LYP Transition-State Structures of the OsX{NH=C(H)C<sub>6</sub>H<sub>4</sub>}( $\eta^2$ -H<sub>2</sub>)(PH<sub>3</sub>)<sub>2</sub> (X = Cl) and the OsH<sub>2</sub>X{NH=C(H)C<sub>6</sub>H<sub>4</sub>}(PH<sub>3</sub>)<sub>2</sub> (X = H) Systems**

	2t-TStN (X = H)	2t-TStC (X = H)	4t-TS (X = Cl)
Os–H(1)	1.721	1.788	1.732
Os–H(2)	1.721	1.667	1.732
Os–X	1.718	1.788	2.565
Os–N	2.098	2.142	2.080
Os–P	2.325	2.316	2.352
N–H <sub>n</sub>	1.016	1.018	1.018
H(1)–H(2)	0.906	2.442	0.891
H(1)–X	2.465	0.869	3.192
H(2)–X	2.465	2.442	3.192
H(1)–Os–X	91.6	28.1	94.0
H(1)–Os–H(2)	30.5	89.9	29.8
H(1)–Os–N	162.7	95.1	164.1
H(1)–Os–C(3)	94.1	164.0	95.5
X–Os–H(2)	91.6	89.9	94.0
X–Os–N	96.7	95.1	91.6
X–Os–C(3)	174.1	164.0	170.2
H(2)–Os–N	162.7	174.9	164.1
H(2)–Os–C(3)	94.1	97.9	95.5
N–Os–C(3)	77.4	77.0	78.6
N–Os–P	88.2	99.5	88.3
C(3)–Os–P	99.1	85.9	95.8
P–Os–P	160.2	157.0	167.1

Despite the geometrical similarity of the two transition states, the activation barriers for the two processes are very different, in agreement with the spectra shown in Figure 1. The transition state **2t-TStN**, in which the dihydrogen ligand lies *trans* to the nitrogen atom, is found 20.1 kcal mol<sup>-1</sup> above the trihydride minimum, whereas **2t-TStC**, in which the dihydrogen ligand is *trans* to the ortho-metallated phenyl ring, is only 12.3 kcal mol<sup>-1</sup> above the minimum.

The motion corresponding to the evolution dihydride–dihydrogen involves the approach of the hydrogen atoms and their estrangement from the metallic center. To understand the origin of the energetic difference between **2t-TStN** and **2t-TStC**, we have optimized the geometry of **2t** with a H(1)–H(3) distance of 0.90 Å, a value very close to that found in **2t-TStC**, but imposed the coplanarity of the OsH<sub>3</sub> unit. This structure is 5.3 kcal mol<sup>-1</sup> above the minimum. The structure of **2t** with a H(1)–H(2) distance of 0.90 Å is 10.5 kcal mol<sup>-1</sup> above the minimum. Thus, the difference in energy between the transition states is already found between the two dihydrogen structures before the twist. It is clear that the approach of H(1) to H(3) is easier than that of H(1) to H(2).

An energy decomposition analysis<sup>20</sup> is also useful in understanding where the difference comes from. In the planar hydride–dihydrogen structures the energies of the two MHL<sub>4</sub> fragments are very different. The fragment OsH{NH=C(H)C<sub>6</sub>H<sub>4</sub>}(PH<sub>3</sub>)<sub>2</sub> with the hydride *trans* to C lies 18 kcal mol<sup>-1</sup> above the same fragment with the hydride *trans* to N, and although the first fragment interacts more strongly with the H–H unit

(20) We consider the species MHL<sub>4</sub>( $\eta^2$ -H<sub>2</sub>) at a particular value of the H–H distance between 0.80 and 1.80 Å has been built from two separate fragments (the H<sub>2</sub> molecule and the MHL<sub>4</sub> fragment), each one at its equilibrium geometry. Thus, the process to obtain MHL<sub>4</sub>( $\eta^2$ -H<sub>2</sub>) at each hydrogen–hydrogen distance can be decomposed into three terms,  $\Delta E_{\text{stret}}(\text{H}_2)$ ,  $\Delta E_{\text{def}}(\text{MHL}_4)$ , and  $\Delta E_{\text{int}}$ , and at each point the variation in the total energy ( $\Delta E_{\text{tot}}$ ) can be obtained by adding the three contributions:  $\Delta E_{\text{tot}} = \Delta E_{\text{stret}}(\text{H}_2) + \Delta E_{\text{def}}(\text{MHL}_4) + \Delta E_{\text{int}}$ .

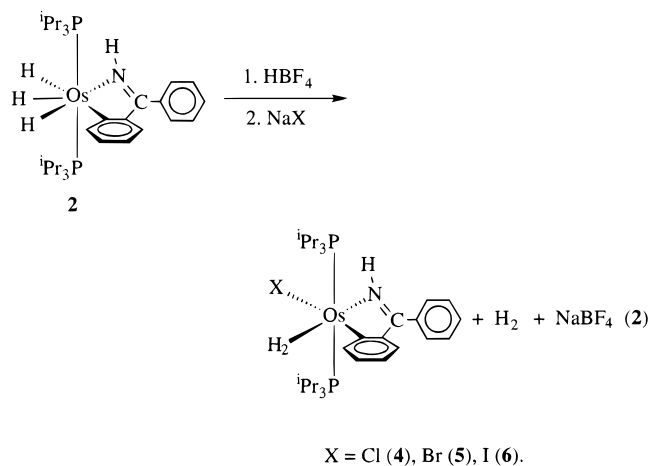
( $\Delta E_{\text{int}} = -49.6 \text{ kcal mol}^{-1}$ ) than does the second one ( $\Delta E_{\text{int}} = -36.8 \text{ kcal mol}^{-1}$ ), the term does not balance the intrafragment destabilization.

Once a dihydrogen structure has been reached, the energies associated with their rotations are similar (7 kcal mol<sup>-1</sup> for the dihydrogen *trans* to C, and 9.6 kcal mol<sup>-1</sup> for the dihydrogen *trans* to N). These energies mainly come from the loss of the metal–dihydrogen interaction in the transition states, with respect to the planar hydrido–dihydrogen structures. For instance, this interaction, which is  $-49.6 \text{ kcal mol}^{-1}$  when the dihydrogen unit H(1)–H(2) is in the equatorial plane, diminishes to  $-39.1 \text{ kcal mol}^{-1}$  in **2t-TStN**.

**2. OsX{NH=C(Ph)C<sub>6</sub>H<sub>4</sub>}( $\eta^2$ -H<sub>2</sub>)(P<sup>i</sup>Pr<sub>3</sub>)<sub>2</sub> (X = Cl, Br, I).** According to the charge which each hydride ligand of **2** bears, it seems to be clear that in the site *trans* to the C atom of the metalated group less electron density is transferred from the ligand to the metal. Therefore, one should expect that an electronegative ligand will prefer to occupy this position. To confirm this, we carried out the reaction of **2** with HCl. In this context, it should be mentioned that a general procedure to generate hydride–halide compounds is the treatment of polyhydride precursors with hydrohalic acids.<sup>21</sup>

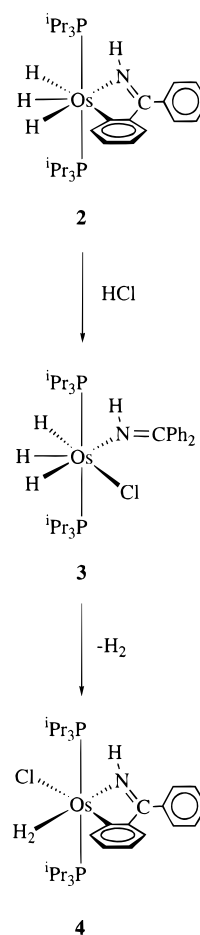
Complex **2** reacts at room temperature with HCl in toluene to give OsH<sub>3</sub>Cl(NH=CPh<sub>2</sub>)(P<sup>i</sup>Pr<sub>3</sub>)<sub>2</sub> (**3**), which can be isolated at  $-78 \text{ }^\circ\text{C}$  as an orange solid in 35% yield. In methanol, complex **3** is unstable and rapidly evolves into OsCl{NH=C(Ph)C<sub>6</sub>H<sub>4</sub>}( $\eta^2$ -H<sub>2</sub>)(P<sup>i</sup>Pr<sub>3</sub>)<sub>2</sub> (**4**), by loss of molecular hydrogen. In toluene at room temperature, complex **3** is stable. However, at  $60 \text{ }^\circ\text{C}$ , it quantitatively affords **4** after 2 weeks (Scheme 1).

Complex **4** can be also synthesized by protonation of a dichloromethane solution of **2** with HBF<sub>4</sub> and subsequent treatment with NaCl in methanol. By this procedure, complex **4** was obtained in 77% yield. Similarly to **4** the complexes OsX{NH=C(Ph)C<sub>6</sub>H<sub>4</sub>}( $\eta^2$ -H<sub>2</sub>)(P<sup>i</sup>Pr<sub>3</sub>)<sub>2</sub> (X = Br (**5**), I (**6**)) can be obtained in 80% yield by treatment of the resulting solution from the protonation of **2**, with methanol solutions of NaBr and NaI, respectively (eq 2).



The spectroscopic data for **3** are consistent with the structure proposed for this complex in Scheme 1. The

Scheme 1



IR spectrum in Nujol shows the  $\nu(\text{N-H})$  vibration at  $3321 \text{ cm}^{-1}$  and the absorptions due to the Os–H bonds at  $2176$  and  $2122 \text{ cm}^{-1}$ . In the <sup>13</sup>C{<sup>1</sup>H} NMR spectrum, the resonance due to the C=N carbon atom appears at  $169.6 \text{ ppm}$  as a triplet with a P–C coupling constant of  $2.6 \text{ Hz}$ . The <sup>31</sup>P{<sup>1</sup>H} NMR spectrum in toluene-*d*<sub>8</sub>, which is temperature-invariant, shows a singlet at  $27.2 \text{ ppm}$ . In the <sup>1</sup>H NMR spectrum, at room temperature, the NH resonance is observed at  $12.42 \text{ ppm}$ . In the high-field region, the spectrum contains a broad resonance at  $-11.97 \text{ ppm}$ . This spectrum is temperature-dependent. Between  $253$  and  $243 \text{ K}$ , a decoalescence of the hydride resonance takes place, and two broad resonances at about  $-9$  (1H) and  $-13$  (2H) ppm are observed. Although a second decoalescence does not occur between  $243$  and  $193 \text{ K}$ , lowering the sample temperature leads to a broadening of the resonance at about  $-13 \text{ ppm}$ . These observations suggest that, similarly to the hydride ligands of **2**, the hydride ligands of **3** undergo two thermally activated site exchange processes, one of them faster than the other one.

The *T*<sub>1</sub> values of the hydride ligands of the OsH<sub>3</sub> unit of **3** were also determined over the temperature range  $293$ – $193 \text{ K}$ . *T*<sub>1</sub>(min) values of  $78$  and  $82 \text{ ms}$  were obtained at  $233 \text{ K}$ . These values support the trihydride character of **3**.

The spectroscopic data for **4**–**6** also support the structure proposed in eq 2. The IR spectra show the  $\nu(\text{NH})$  band at about  $3330 \text{ cm}^{-1}$ . The presence of the ortho-metalated benzophenone imine group is also supported by the <sup>13</sup>C{<sup>1</sup>H} NMR spectra, which contain

(21) Hlatky, G. G.; Crabtree, R. H. *Coord. Chem. Rev.* **1985**, *65*, 1.

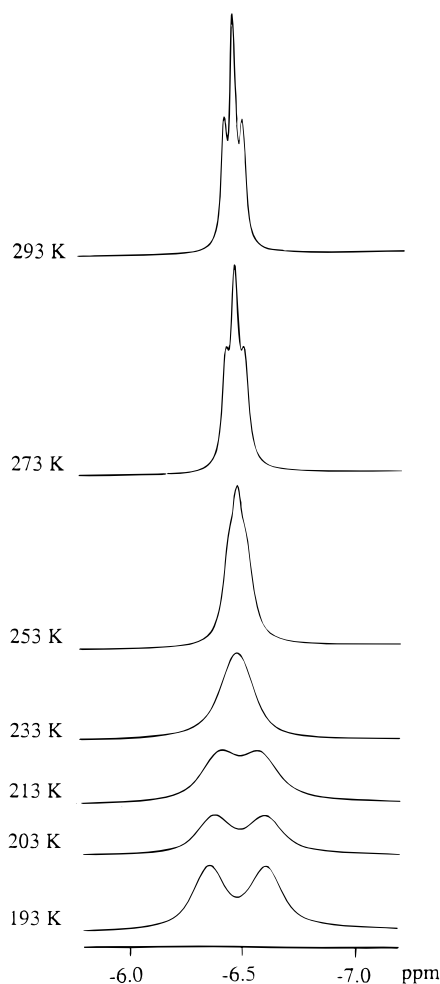


**Figure 5.** Variable-temperature  $^1\text{H}$  NMR spectra (300 MHz, toluene- $d_8$ ) in the high-field region of  $\text{OsCl}\{\text{NH}=\text{C}(\text{Ph})\text{C}_6\text{H}_4\}(\eta^2\text{-H}_2)(\text{P}^i\text{Pr}_3)_2$  (**4**).

triplets at about 177 ( $J(\text{PC}) = 2.8$  Hz) and 173 ( $J(\text{PC}) \approx 5$  Hz) ppm, assigned to the C=N and Os–C carbon atoms, respectively. The  $^{31}\text{P}\{^1\text{H}\}$  NMR spectra of the three compounds, which are temperature-invariant, show singlets at 6.8 (**4**), 3.3 (**5**), and  $-2.2$  (**6**) ppm. Under off-resonance conditions, they are split into triplets. At room temperature, in dichloromethane- $d_2$  as solvent, the  $^1\text{H}$  NMR spectra contain a broad NH resonance at about 10.8 ppm, and in the high-field region double triplets at  $-6.52$  ( $J(\text{PH}) = 12.9$  Hz,  $J(\text{HH}) = 2.7$  Hz; **4**),  $-6.99$  ( $J(\text{PH}) = 12.7$  Hz,  $J(\text{HH}) = 3.0$  Hz; **5**), and  $-7.93$  ( $J(\text{PH}) = 12.7$  Hz,  $J(\text{HH}) = 2.9$  Hz; **6**) ppm correspond to the  $\text{H}_2$  unit. The multiplicity of these resonances is the result of the nuclear spin coupling between the dihydrogen ligands and the phosphorus and NH nuclei. The nuclear spin coupling between the dihydrogen ligand and the NH proton was confirmed by  $^1\text{H}$ -COSY NMR experiments.

In contrast to the  $^{31}\text{P}\{^1\text{H}\}$  NMR spectra, the  $^1\text{H}$  NMR spectra are temperature-dependent. The three compounds display the same behavior. Figure 5 shows the  $^1\text{H}$  NMR spectrum of **4** in the high-field region as a function of the temperature, in toluene- $d_8$  as solvent, where the  $J(\text{HH})$  coupling constant is not observed. Lowering the sample temperature leads to broadening of the resonance. At very low temperature (213 K)

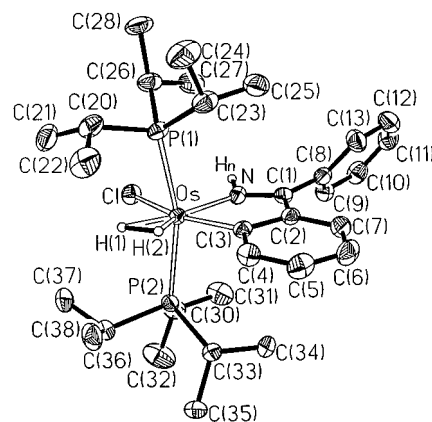


**Figure 6.** Molecular diagram of  $\text{OsCl}\{\text{NH}=\text{C}(\text{Ph})\text{C}_6\text{H}_4\}(\eta^2\text{-H}_2)(\text{P}^i\text{Pr}_3)_2$  (**4**). Thermal ellipsoids are shown at 50% probability.

decoalescence occurs and, at 193 K, two signals are clearly observed.

The  $T_1$  values of the high-field-region resonances were determined over the temperature range 213–293 K. The  $T_1$  (min) values for the three compounds, **49** (**4**) and **50** (**5** and **6**) ms, occur at the same temperature (233 K). These values correspond to hydrogen–hydrogen distances of 1.08 Å (fast spinning) or 1.36 Å (slow spinning).<sup>1f</sup>

The partially deuterated dihydrogen derivatives  $\text{OsX}\{\text{NH}=\text{C}(\text{Ph})\text{C}_6\text{H}_4\}(\eta^2\text{-HD})(\text{P}^i\text{Pr}_3)_2$  ( $\text{X} = \text{Cl}$  (**4-d**),  $\text{Br}$  (**5-d**), and  $\text{I}$  (**6-d**)) were prepared according to eq 2 using methanol- $d_4$  instead of methanol. They have H–D coupling constants of 6.3 (**4-d**), 6.6 (**5-d**), and 6.8 (**6-d**) Hz. According to eq 3, these values allow us to calculate a separation between the hydrogen atoms of the dihydrogen ligands of **4–6** of 1.31 Å, suggesting that the coordinated hydrogen molecules in these derivatives are in a slow-rotation regime, in agreement with the observed decoalescence.

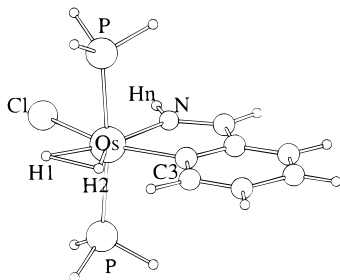
$$d(\text{H}-\text{H}) = -0.0167[J(\text{HD})] + 1.42 \quad (3)$$

The X-ray diffraction study on a single crystal of **4** confirms the structure proposed for **4–6** in eq 2. A view of the molecular geometry of **4** is shown in Figure 6. Selected bond distances and angles are listed in Table 4. The hydrogen atoms H(1) and H(2) were located in the difference Fourier maps and refined as isotropic atoms together with the rest of the non-hydrogen atoms of the structure, giving Os–H(1) and Os–H(2) distances of 1.53(4) and 1.42(4) Å, respectively. The H(1)–H(2) distance is 1.22(5) Å.

The osmium atom is coordinated in a somewhat octahedral fashion with the two triisopropylphosphine ligands in *trans* positions ( $\text{P}(1)\text{--Os--P}(2) = 162.31(4)^\circ$ ). An ideal equatorial plane is formed by the atoms C(3) and N of the ortho-metalated benzophenone imine group coordinating with the osmium atom to form a five-membered ring ( $\text{C}(3)\text{--Os--N} = 75.1(1)^\circ$ ) and the chloro and dihydrogen ligands, which align along the Cl–M–C axis, *cis*-disposed. The five-membered metallacycle is almost planar. The deviations from the best plane are  $-0.0001(2)$  (Os),  $-0.036(4)$  (C(1)),  $0.007(4)$  (C(2)),  $0.011(4)$  (C(3)), and  $0.027(4)$  (N) Å.

**Table 4.** Selected Bond Distances (Å) and Angles (deg) for the Complex

OsCl{NH=C(Ph)C <sub>6</sub> H <sub>4</sub> }(η <sup>2</sup> -H <sub>2</sub> )(P <sup>i</sup> Pr <sub>3</sub> ) <sub>2</sub> ( <b>4</b> )			
Os–H(1)	1.53(4)	N–C(1)	1.291(5)
Os–H(2)	1.42(4)	C(1)–C(2)	1.451(5)
Os–Cl	2.482(1)	C(1)–C(8)	1.484(6)
Os–P(1)	2.387(1)	C(2)–C(3)	1.431(6)
Os–P(2)	2.3806(9)	C(3)–C(4)	1.417(5)
Os–N	2.097(3)	N–H <sub>n</sub>	0.96
Os–C(3)	2.069(4)	Cl–H <sub>n</sub>	2.81
H(1)–H(2)	1.22(5)	Cl–H(1)	2.72(4)
Cl–Os–P(1)	87.88(3)	P(2)–Os–H(2)	88(1)
Cl–Os–P(2)	87.92(3)	N–Os–C(3)	75.1(1)
Cl–Os–N	82.48(9)	N–Os–H(1)	164(1)
Cl–Os–C(3)	157.5(1)	N–Os–H(2)	147(2)
Cl–Os–H(1)	82(1)	C(3)–Os–H(1)	121(1)
Cl–Os–H(2)	130(2)	C(3)–Os–H(2)	72(2)
P(1)–Os–P(2)	162.31(4)	H(1)–Os–H(2)	49(2)
P(1)–Os–N	96.32(8)	Os–N–C(1)	121.7(3)
P(1)–Os–C(3)	96.29(9)	N–C(1)–C(2)	112.8(4)
P(1)–Os–H(1)	82(1)	N–C(1)–C(8)	121.9(3)
P(1)–Os–H(2)	82(1)	C(1)–C(2)–C(3)	114.1(3)
P(2)–Os–N	100.15(8)	Os–C(3)–C(2)	116.2(2)
P(2)–Os–C(3)	94.15(9)	Os–C(3)–C(4)	129.5(3)
P(2)–Os–H(1)	80(1)	C(2)–C(3)–C(4)	114.2(4)

**Figure 7.** Optimized structure of OsCl{NH=C(H)C<sub>6</sub>H<sub>4</sub>}(η<sup>2</sup>-H<sub>2</sub>)(PH<sub>3</sub>)<sub>2</sub> (**4t**).

The Os–N bond length of 2.097(3) Å and the Os–C(3) bond distance of 2.069 Å are typical for Os–N and Os–C(aryl) single bonds, respectively, and are in agreement with the values previously found for the complexes Os–(C<sub>2</sub>Ph){NH=C(Ph)C<sub>6</sub>H<sub>4</sub>}(CO)(P<sup>i</sup>Pr<sub>3</sub>)<sub>2</sub> (2.106(7) and 2.089–(7) Å),<sup>12</sup> Os{NH=C(Ph)C<sub>6</sub>H<sub>4</sub>}(η<sup>6</sup>-C<sub>6</sub>H<sub>3</sub>Me<sub>3</sub>)(P<sup>i</sup>Pr<sub>3</sub>)]PF<sub>6</sub> (2.083(4) and 2.072(4) Å),<sup>22</sup> OsH{(C<sub>6</sub>H<sub>3</sub>-*p*-Me)(*p*-tolyl)-CNNC(*p*-tolyl)<sub>2</sub>}(CO)<sub>2</sub>(PPh<sub>3</sub>) (2.119(5) and 2.100(7) Å),<sup>23</sup> and *fac*-Os{C, *N*-3-Me[2-(MeC<sub>6</sub>H<sub>4</sub>)NCMe<sub>3</sub>]C<sub>6</sub>H<sub>3</sub>}(2-Me-C<sub>6</sub>H<sub>4</sub>)(CN<sup>-</sup>Bu)<sub>3</sub> (2.193(24) and 2.077(20) Å).<sup>24</sup>

We have also carried out a theoretical determination of the structure of complexes **4**–**6**, taking the OsX{NH=C(H)C<sub>6</sub>H<sub>4</sub>}(η<sup>2</sup>-H<sub>2</sub>)(PH<sub>3</sub>)<sub>2</sub> (X = Cl (**4t**), Br (**5t**), I (**6t**)) system as a model. Selected geometrical parameters are collected in Table 1, and the structure of **4t** is shown in Figure 7. Because the three complexes present very similar geometries, we will focus our discussion on **4t**.

Bond distances and angles for the non-hydrogen atoms of **4t** agree well with those determined by X-ray

diffraction for **4**. The main discrepancy is found in the H(1)–H(2) distance (1.483 Å), which is about 0.25 Å longer than that determined from the X-ray diffraction study and is 0.17 Å longer than the hydrogen–hydrogen distance calculated according to eq 3. In this context, it should be mentioned that a recent theoretical study on the elongated dihydrogen complexes [Ru(η<sup>5</sup>-C<sub>5</sub>H<sub>5</sub>)(η<sup>2</sup>-H<sub>2</sub>)(R<sub>2</sub>PCH<sub>2</sub>PR<sub>2</sub>)]<sup>+</sup> has revealed that the experimental H–H distance, determined by a neutron diffraction study, cannot be explained with pure electronic structure results.<sup>71</sup> The main reason lies in the shape of the potential energy surface corresponding to the stretch of the H–H unit of the complex, which is very anharmonic.

Let us analyze structural changes caused in the complexes by the substitution of a hydride ligand (**2t**) by a chloride ligand (**4t**). The most remarkable fact is the diminution of the H(1)–H(2) distance from 1.72 Å (**2t**) to a value that falls in the range of a stretched-dihydrogen complex (1.48 Å) in **4t**. This is in contrast with that previously observed in the complexes *trans*-[RuX(η<sup>2</sup>-H<sub>2</sub>)L<sub>2</sub>]<sup>+</sup><sup>25</sup> and *trans*-[OsX(η<sup>2</sup>-H<sub>2</sub>)L<sub>2</sub>]<sup>+</sup> (X = H, Cl),<sup>2b,f,26</sup> where a change of the *trans* ligand from hydride to chloride increases the H–H distance and the hydride character of the dihydrogen ligand. For instance, the complex *trans*-[OsH(η<sup>2</sup>-H<sub>2</sub>)(dppe)<sub>2</sub>]<sup>+</sup> has a H–H distance of 0.99 Å according to NMR studies,<sup>2b</sup> while neutron diffraction studies of *trans*-[OsCl(η<sup>2</sup>-H<sub>2</sub>)(dppe)<sub>2</sub>]<sup>+</sup> have revealed an elongated H···H ligand with *R*<sub>H–H</sub> = 1.22 Å.<sup>2f</sup> The different behavior of a chloride ligand in *trans* and *cis* positions with respect to a dihydrogen unit can be interpreted by considering that in the *trans* position the strong π-donor nature of Cl dominates, raising the energy of d<sub>π</sub> orbitals and increasing back-donation to the σ\* (H<sub>2</sub>) orbital. On the other hand, in the *cis* position the weak σ-donor character predominates, transferring less electronic density to the metal than a hydride and thus rendering less basic the metal center. Following this analysis, in **4t** less electronic density would be transferred from the metal to the H(1)–H(2) unit that in **2t**. The Bader net atomic charges computed in **4t** for H(1) (–0.18e) and H(2) (–0.15e) reveal that a noticeable diminution (0.10e), with respect to those of the same two atoms in **2t**, has occurred. Charges calculated for H(1) and H(2) in **4t** are very similar to those computed with the same method for the dihydrogen unit of the elongated-dihydrogen complex *trans*-[Os-(HCO<sub>2</sub>)(η<sup>2</sup>-H<sub>2</sub>){NH<sub>2</sub>(CH<sub>2</sub>)<sub>2</sub>NH<sub>2</sub>}]<sup>+</sup> (–0.18e and –0.17e).<sup>18</sup>

At first glance the decoalescence observed in Figure 5 could be due to a restricted rotational motion of the elongated dihydrogen ligand or, alternatively, to a low-energy bond-splitting/bond-forming process. Previously, we have pointed out that for an elongated-dihydrogen compound (also for those with a restricted rotational motion of the dihydrogen ligand) a plot of the potential energy versus the hydrogen–hydrogen distance (*R*<sub>H–H</sub>) should have one minimum at the equilibrium hydrogen–hydrogen distance, while for a low-energy bond-splitting/bond-forming process, a potential surface with a double well must be expected.

(22) Werner, H.; Daniel, T.; Braun, T.; Nürnberg, O. *J. Organomet. Chem.* **1994**, *480*, 145.

(23) Gallop, M. A.; Rickard, C. E. F.; Roper, W. R. *J. Organomet. Chem.* **1990**, *395*, 333.

(24) Arnold, J.; Wilkinson, G.; Hussain, B.; Hurthouse, M. B. *Organometallics* **1989**, *8*, 1362.

(25) Chin, B.; Lough, A. J.; Morris, R. H.; Schweitzer, C. T.; D'Agostino, C. *Inorg. Chem.* **1994**, *33*, 6278.

(26) Mezzetti, A.; Del Zotto, A.; Rigo, P.; Farnetti, E. *J. Chem. Soc., Dalton Trans.* **1991**, 1525.



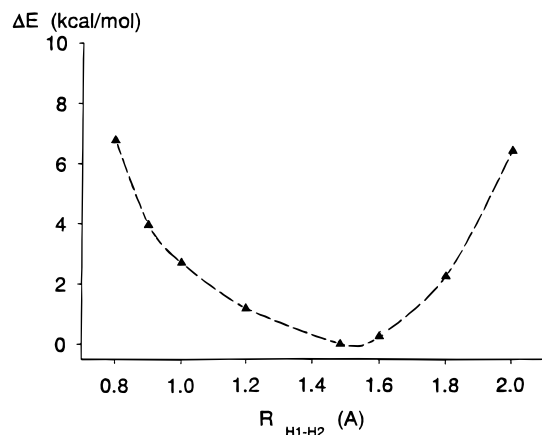


**Figure 8.** Energy profile for the lengthening of the H(1)–H(2) distance in the complex  $\text{OsCl}\{\text{NH}=\text{C}(\text{H})\text{C}_6\text{H}_4\}(\eta^2\text{-H}_2)\text{-}(\text{PH}_3)_2$  (**4t**).

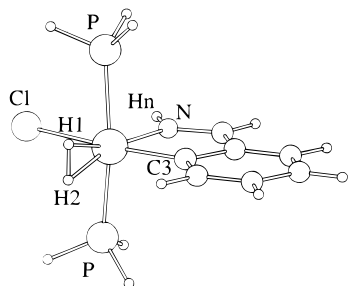


**Figure 9.** Transition-state structure for the hydrogen exchange process in **4t**: **4t-TS**.

To clarify this point, we have calculated the potential energy profile for the H(1)–H(2) stretch in **4t**. According to the curve depicted in Figure 8 the nature of the elongated dihydrogen of the  $\text{H}_2$  unit of **4** is confirmed. Furthermore, since the curve does not have a double well, without the shadow of a doubt, a low-energy bond-splitting/bond-forming process must be totally rejected. The latter is in agreement with the  $\ln T_1$  vs  $1/T$  plot, which has the usual V-shape and does not show any distortion that would be expected for a tautomeric equilibrium, where the ratio of the two tautomers should be temperature-dependent.<sup>28</sup>

The transition state for the hydrogen exchange in **4t** (**4t-TS**) has been located with the same methodology as that used for the other transition states. It also presents a dihydrogen-like nature (H(1)–H(2) = 0.891 Å). Despite the different H(1)–H(2) distances in **2t** and **4t**, the geometry of **4t-TS** (Figure 9, Table 3) is similar to that of **2t-TStN**. However, the hydrogen exchange

takes place in **4t** with an energy barrier<sup>29</sup> of 11.0 kcal mol<sup>-1</sup>, which is substantially lower than in **2t** (20.1 kcal mol<sup>-1</sup>). The explanation for this fact can be found in Figure 8. To cause H(1) and H(2) to approach at a distance of 0.90 Å costs only 4.0 kcal mol<sup>-1</sup> in **4t**, while 10.5 kcal mol<sup>-1</sup> is necessary in **2t**. The presence of a *cis*-chloride ligand instead of a hydride facilitates the approach between H(1) and H(2). Once the dihydrogen ligands are formed, the rotational barriers are similar (7.0 (**4t**) and 9.6 (**2t**) kcal mol<sup>-1</sup>).

## Concluding Remarks

This study has revealed that the hexahydride  $\text{OsH}_6(\text{P}^i\text{Pr}_3)_2$  reacts with benzophenone imine to give the derivative  $\text{OsH}_3\{\text{NH}=\text{C}(\text{Ph})\text{C}_6\text{H}_4\}(\text{P}^i\text{Pr}_3)_2$  containing three hydride ligands and a bidentate group in the equatorial plane of a pentagonal-bipyramidal arrangement of ligands around the metallic center. In solution two thermally activated exchange processes take place between the hydride ligands, one of them faster than the other one. The slower exchange process involves the hydride ligand disposed *trans* to the nitrogen atom and the central hydride ligand, while the faster one takes place between the latter and that located *trans* to the ortho-metalated phenyl ring.

In the transition state of both processes, the exchanging atoms form a dihydrogen unit, which is twisted 90° with regard to the position of the minimum. The difference in energy between them is a consequence of the difference in energy needed for the exchanging atoms to approach before the twist.

In the site *trans* to the phenyl ring of the metalated group of **2**, less electron density is transferred from the ligand to the metal. In agreement with this, the hydride ligand located in this position can be replaced by electronegative ligands such as chloride, bromide, and iodide. This change of ligands produces significant disruptions in the interaction between the other two hydrogen ligands and the osmium atom. Thus, in the new compounds,  $\text{OsX}\{\text{NH}=\text{C}(\text{Ph})\text{C}_6\text{H}_4\}(\eta^2\text{-H}_2)(\text{P}^i\text{Pr}_3)_2$ , the  $\text{H}_2$  unit forms an elongated dihydrogen ligand, which in solution shows a restricted rotational motion. The transition states for the hydrogen exchange in these compounds also present a dihydrogen-like nature.

In conclusion, the ligand X of the complexes  $\text{OsX}\{\text{NH}=\text{C}(\text{Ph})\text{C}_6\text{H}_4\}\text{H}_2(\text{P}^i\text{Pr}_3)_2$  determines the nature of the  $\text{H}_2$  unit and, as a consequence, the energy barrier for the rotational motion of the  $\text{H}_2$  unit in solution.

## Experimental Section

**Physical Measurements.** Infrared spectra were recorded as Nujol mulls on polyethylene sheets using a Nicolet 550 spectrometer. NMR spectra were recorded on a Varian UNITY 300, Varian GEMINI 2000 300 MHz, or on a Bruker ARX 300. The probe temperature of the NMR spectrometers was calibrated at each temperature against a methanol standard in the range 293–193 K and against ethylene glycol in the range 353–303 K. For the  $T_1$  measurements the 180° pulses were calibrated at each temperature. <sup>1</sup>H and <sup>13</sup>C{<sup>1</sup>H} chemical

(27) At each fixed value of  $R_{\text{H-H}}$  the rest of the geometrical parameters have been optimized at the B3LYP level.

(28) (a) Kubas, G. J.; Unkefer, C. J.; Swanson, B. I.; Fukushima, E. *J. Am. Chem. Soc.* **1986**, *108*, 7000. (b) Kubas, G. J.; Ryan, R. R.; Unkefer, C. J. *J. Am. Chem. Soc.* **1987**, *109*, 8113. (c) Conroy-Lewis, F. M.; Simpson, S. J. *J. Am. Chem. Soc., Chem. Commun.* **1987**, 1675. (d) Chinn, M. S.; Heinekey, D. M. *J. Am. Chem. Soc.* **1987**, *109*, 5865. (e) Chinn, M. S.; Heinekey, D. M.; Payne, N. G.; Sofield, C. D. *Organometallics* **1989**, *8*, 1824. (f) Cappellani, E. P.; Maltby, P. A.; Morris, R. H.; Schweitzer, C. T.; Steele, M. R. *Inorg. Chem.* **1989**, *28*, 4437. (g) Arliguie, T.; Chaudret, B. *J. Chem. Soc., Chem. Commun.* **1989**, 155. (h) Khalsa, G. R. K.; Kubas, G. J.; Unkefer, C. J.; Van Der Sluys, L. S.; Kubat-Martin, K. A. K. *J. Am. Chem. Soc.* **1990**, *112*, 189. (i) Luo, X.-L.; Crabtree, R. H. *J. Am. Chem. Soc.* **1990**, *112*, 6912. (j) Luo, X.-L.; Crabtree, R. H. *J. Am. Chem. Soc.* **1990**, *112*, 6912. (k) Luo, X.-L.; Michos, D.; Crabtree, R. H. *Organometallics* **1992**, *11*, 237.

(29) The value of  $\Delta G_{293}^\ddagger$  estimated by NMR spectroscopy for the rotation of the  $\text{H}_2$  unit in **4** is 12 kcal mol<sup>-1</sup>.

shifts were measured relative to partially deuterated solvent peaks but are reported relative to tetramethylsilane.  $^{31}\text{P}\{^1\text{H}\}$  chemical shifts are reported relative to  $\text{H}_3\text{PO}_4$  (85%). The coupling constants  $J$  and  $N$  ( $N = J(\text{PH}) + J(\text{P}'\text{H})$  for  $^1\text{H}$  and  $N = J(\text{PC}) + J(\text{P}'\text{C})$  for  $^{13}\text{C}\{^1\text{H}\}$ ) are given in hertz. C, H, and N analyses were carried out in a Perkin-Elmer 2400 CHNS/O analyzer. Mass spectral analyses were performed with a VG Auto Spec instrument. The ions were produced (FAB<sup>+</sup> mode) with the standard Cs<sup>+</sup> gun at ca. 30 kV, and 3-nitrobenzyl alcohol (NBA) was used as the matrix.

**Synthesis.** All reactions were carried out with exclusion of air using standard Schlenk techniques. Solvents were dried by known procedures and distilled under argon prior to use. The complex  $\text{OsH}_2\text{Cl}_2(\text{P}^i\text{Pr}_3)_2$  was prepared according to the literature method.<sup>30</sup>

**Kinetic Analysis.** Complete line shape analysis of the  $^1\text{H}\{^{31}\text{P}\}$  NMR spectra of **2** was achieved using the program DNMR6 (QCPE, Indiana University). The rate constants for various temperatures were obtained by visually matching observed and calculated spectra. In the temperature range 213–243 K the rate for the site exchange process H(1)–H(2) was fixed at  $0\text{ s}^{-1}$ , and the resonance corresponding to the H(2) hydride ligand was used to estimate the  $T_2$  value. The rate values obtained for the site exchange process H(1)–H(3) were extrapolated for the rest of the temperature values (253–353 K). With these rate values the  $T_2$  value was estimated and the rates for the site exchange process H(1)–H(2) at each point of the temperature range 253–353 K were computed. The activation parameters  $\Delta H^\ddagger$  and  $\Delta S^\ddagger$  were calculated by a least-squares fit of  $\ln(k/T)$  vs  $1/T$  (Eyring equation). Error analysis assumed a 10% error in the rate constant and 1 K error in the temperature. Errors were computed by published methods.<sup>31</sup>

**Preparation of  $\text{OsH}_3\{\text{NH}=\text{C}(\text{Ph})\text{C}_6\text{H}_4\}(\text{P}^i\text{Pr}_3)_2$  (**2**).** A suspension of  $\text{OsH}_2\text{Cl}_2(\text{P}^i\text{Pr}_3)_2$  (200 mg, 0.35 mmol) in 16 mL of toluene was first treated with  $\text{NaBH}_4$  (133 mg, 3.5 mmol) and then dropwise with 1.0 mL of methanol. After it was stirred for 15 min at room temperature, the solution was filtered through Kieselguhr and concentrated to dryness. The white residue obtained was dissolved in 10 mL of toluene and treated with 74.5 mg (0.42 mmol) of benzophenone imine. The sample was heated under reflux for 6 h. The resulting red solution was filtered by Kieselguhr and concentrated to dryness. Addition of methanol caused the precipitation of a red solid, which was separated by decantation, washed with methanol, and dried in vacuo: yield 193.3 mg (80%). IR (Nujol):  $\nu(\text{NH})$  3348  $\text{cm}^{-1}$ ,  $\nu(\text{OsH})$  2143, 2106, 1942  $\text{cm}^{-1}$ .  $^1\text{H}$  NMR (300 MHz,  $\text{C}_6\text{D}_6$ , 293 K):  $\delta$  10.25 (br, 1 H, NH), 8.93 [d,  $J(\text{HH}) = 7.5$  Hz, 1 H, Ph], 7.68 [d,  $J(\text{HH}) = 7.5$  Hz, 1 H, Ph], 7.47 (m, 2 H, Ph), 7.17–6.93 (m, 5 H, Ph), 1.82 (m, 6 H, PCH), 1.01 [dvt,  $N = 12.6$  Hz,  $J(\text{HH}) = 6.9$  Hz, 18 H,  $\text{PCCH}_3$ ], 0.98 [dvt,  $N = 12.6$  Hz,  $J(\text{HH}) = 6.9$  Hz, 18 H,  $\text{PCCH}_3$ ], –9.07 (br, 2 H,  $\text{OsH}_3$ ), –9.87 (br, 1 H,  $\text{OsH}_3$ ).  $^{31}\text{P}\{^1\text{H}\}$  NMR (121.42 MHz,  $\text{C}_6\text{D}_6$ , 293 K):  $\delta$  26.8 (s).  $^{13}\text{C}\{^1\text{H}\}$  NMR (75.42 MHz,  $\text{C}_6\text{D}_6$ , 293 K):  $\delta$  194.6 [t,  $J(\text{PC}) = 5.6$  Hz,  $\text{Os}-\text{C}$ ], 179.9 [t,  $J(\text{PC}) = 3.0$  Hz,  $\text{N}=\text{C}$ ], 147.4, 142.4, 140.2, 130.8, 128.9, 128.4, 128.3, 118.3 (all s, Ph), 27.7 (vt,  $N = 25.6$  Hz, PCH), 20.1, 19.9 (both s,  $\text{PCCH}_3$ ). Anal. Calcd for  $\text{C}_{31}\text{H}_{55}\text{NOsP}_2$ : C, 53.66; H, 7.98; N, 2.01. Found: C, 53.25; H, 7.46; N, 2.00.  $T_1$  (ms,  $\text{OsH}_3$ , 300 MHz,  $\text{C}_7\text{D}_8$ ): 283, 312 (283 K), 198, 182 (253 K), 102, 124, 129 (233 K), 99, 117, 105 (228 K), 89, 114, 90 (223 K), 98, 119, 100 (218 K), 107, 121, 106 (213 K), 179, 182, 167 (198 K).

**Preparation of  $\text{OsH}_3\text{Cl}(\text{NH}=\text{CPh}_2)(\text{P}^i\text{Pr}_3)_2$  (**3**).** A solution of **2** (100 mg, 0.14 mmol) in 10 mL of toluene was treated with 1.2 mL (0.14 mmol) of a toluene–0.12 M HCl solution. After the mixture was stirred for 30 min at room temperature,

the resulting orange solution was filtered through Kieselguhr and concentrated to dryness. Ten milliliters of pentane was added and evaporated until an orange solid began to precipitate. The suspension was stored at  $-78^\circ\text{C}$  for 1 h, and the orange solid obtained was separated by decantation and dried in vacuo: yield 36.1 mg (35%). IR (Nujol):  $\nu(\text{NH})$  3321  $\text{cm}^{-1}$ ,  $\nu(\text{OsH})$  2176, 2122  $\text{cm}^{-1}$ .  $^1\text{H}$  NMR (300 MHz,  $\text{C}_6\text{D}_6$ , 293 K):  $\delta$  12.42 (br, 1 H, NH), 7.71 (m, 2 H, Ph), 7.66 (m, 2 H, Ph), 7.24 (m, 1 H, Ph), 7.12 (m, 1 H, Ph), 6.93 (m, 4 H, Ph), 2.18 (m, 6 H, PCH), 1.29 [dvt,  $N = 13.2$  Hz,  $J(\text{HH}) = 6.9$  Hz, 18 H,  $\text{PCCH}_3$ ], 0.93 [dvt,  $N = 12.6$  Hz,  $J(\text{HH}) = 6.9$  Hz, 18 H,  $\text{PCCH}_3$ ], –11.97 (br, 3 H,  $\text{OsH}_3$ ).  $^{31}\text{P}\{^1\text{H}\}$  NMR (121.42 MHz,  $\text{C}_6\text{D}_6$ , 293 K):  $\delta$  27.2 (s).  $^{13}\text{C}\{^1\text{H}\}$  NMR (75.42 MHz,  $\text{C}_6\text{D}_6$ , 293 K):  $\delta$  169.6 [t,  $J(\text{PC}) = 2.6$  Hz,  $\text{N}=\text{C}$ ], 140.1, 138.6, 130.7, 130.0, 129.8, 129.5, 129.2, 127.7, 127.3 (all s, Ph), 24.7 [vt,  $N = 23.4$  Hz, PCH], 20.6, 19.5 (both s,  $\text{PCCH}_3$ ). Anal. Calcd for  $\text{C}_{31}\text{H}_{56}\text{ClNOsP}_2$ : C, 50.97; H, 7.72; N, 1.91. Found: C, 50.62; H, 7.42; N, 1.84.  $T_1$  (ms,  $\text{OsH}_3$ , 300 MHz,  $\text{C}_7\text{D}_8$ ): 165 (293 K), 93 (253 K), 78, 82 (233 K), 92, 96 (213 K), 197, 224 (193 K).

**Preparation of  $\text{OsCl}\{\text{NH}=\text{C}(\text{Ph})\text{C}_6\text{H}_4\}(\eta^2\text{-H}_2)(\text{P}^i\text{Pr}_3)_2$  (**4**).** A solution of **2** (120 mg, 0.17 mmol) in 5 mL of  $\text{CH}_2\text{Cl}_2$  was treated with  $\text{HBF}_4$  (23.5  $\mu\text{L}$ , 0.17 mmol). The resulting red solution obtained was evaporated to dryness, and the residue was treated with a solution of NaCl (16.4 mg, 0.17 mmol) in 8 mL of methanol. The red solid obtained was separated by decantation, washed with methanol, and dried in vacuo: yield 97.1 mg (77%). IR (Nujol):  $\nu(\text{NH})$  3329  $\text{cm}^{-1}$ ,  $\nu(\text{OsH})$  2251, 2160  $\text{cm}^{-1}$ .  $^1\text{H}$  NMR (300 MHz,  $\text{CD}_2\text{Cl}_2$ , 293 K):  $\delta$  10.8 (br, 1 H, NH), 7.86 (m, 1 H, Ph), 7.58–7.50 (m, 5 H, Ph), 7.35 (m, 1 H, Ph), 6.75 (m, 2 H, Ph), 2.92 (m, 6 H, PCH), 1.16 [dvt,  $N = 12.7$  Hz,  $J(\text{HH}) = 7.0$  Hz, 18 H,  $\text{PCCH}_3$ ], 0.95 [dvt,  $N = 12.6$  Hz,  $J(\text{HH}) = 6.9$  Hz, 18 H,  $\text{PCCH}_3$ ], –6.52 [td,  $J(\text{PH}) = 12.9$  Hz,  $J(\text{H}-\text{NH}) = 2.7$  Hz, 2 H,  $\text{OsH}_2$ ].  $^{31}\text{P}\{^1\text{H}\}$  NMR (121.42 MHz,  $\text{CD}_2\text{Cl}_2$ , 293 K):  $\delta$  6.8 (s, t in off-resonance).  $^{13}\text{C}\{^1\text{H}\}$  NMR (75.42 MHz,  $\text{CD}_2\text{Cl}_2$ , 293 K):  $\delta$  176.0 [t,  $J(\text{PC}) = 2.8$  Hz,  $\text{N}=\text{C}$ ], 172.8 [t,  $J(\text{PC}) = 5.0$  Hz,  $\text{Os}-\text{C}$ ], 145.8, 143.8, 138.0, 130.6, 130.5, 129.7, 129.1, 128.7, 118.3 (all s, Ph), 24.7 (vt,  $N = 24.8$  Hz, PCH), 19.6, 19.0 (both s,  $\text{PCCH}_3$ ). Anal. Calcd for  $\text{C}_{31}\text{H}_{54}\text{ClNOsP}_2$ : C, 51.11; H, 7.47; N, 1.92. Found: C, 50.81; H, 7.37; N, 1.87. MS (FAB<sup>+</sup>):  $m/e$  727 ( $\text{M}^+ - 2\text{H}$ ).  $T_1$  [ms,  $\text{Os}(\eta^2\text{-H}_2)$ , 300 MHz,  $\text{C}_7\text{D}_8$ ]: 127 (293 K), 92 (273 K), 66 (253 K), 51 (238 K), 49 (233 K), 58, 61 (223 K), 67, 69 (213 K).

**Preparation of  $\text{OsCl}\{\text{NH}=\text{C}(\text{Ph})\text{C}_6\text{H}_4\}(\eta^2\text{-HD})(\text{P}^i\text{Pr}_3)_2$  (**4-d**) and  $\text{OsCl}\{\text{NH}=\text{C}(\text{Ph})\text{C}_6\text{H}_4\}(\eta^2\text{-D}_2)(\text{P}^i\text{Pr}_3)_2$  (**4-d2**).** A suspension of **2** (35 mg, 0.05 mmol) in 3 mL of MeOD was treated first with  $\text{HBF}_4$  (7.1  $\mu\text{L}$ , 0.05 mmol). After 10 min, a solution of NaCl (4.4 mg, 0.05 mmol) in 3 mL of MeOD was added to the red solution obtained. The red solid formed was separated by decantation and dried in vacuo.  $^1\text{H}\{^{31}\text{P}\}$  NMR (300 MHz,  $\text{CD}_2\text{Cl}_2$ , 293 K):  $\delta$  –6.51 [td,  $J(\text{HD}) = 6.3$  Hz,  $J(\text{H}-\text{NH}) = 2.7$  Hz,  $\text{OsHD}$ ].

**Reaction of **4** with  $\text{NaBH}_4$ .** A solution of **4** (75 mg, 0.10 mmol) in 10 mL of toluene was first treated with  $\text{NaBH}_4$  (38.8 mg, 1.02 mmol) and then dropwise with 0.8 mL of methanol. After it was stirred at room temperature for 20 min, the sample was filtered through Kieselguhr and concentrated to dryness. The addition of methanol caused the precipitation of a red solid, which was separated by decantation, washed with methanol, and dried in vacuo. The red solid obtained was characterized as **2** by  $^1\text{H}$  and  $^{31}\text{P}$  NMR spectroscopy. Yield: 63 mg (83%).

**Preparation of  $\text{OsBr}\{\text{NH}=\text{C}(\text{Ph})\text{C}_6\text{H}_4\}(\eta^2\text{-H}_2)(\text{P}^i\text{Pr}_3)_2$  (**5**).** A solution of **2** (100 mg, 0.14 mmol) in 5 mL of  $\text{CH}_2\text{Cl}_2$  was treated with  $\text{HBF}_4$  (19.6  $\mu\text{L}$ , 0.14 mmol). The resulting red solution obtained was evaporated to dryness, and the residue was treated with a solution of NaBr (23.0 mg, 0.14 mmol) in 8 mL of methanol. The red solid obtained was separated by decantation, washed with methanol, and dried

(30) Aracama, M.; Esteruelas, M. A.; Lahoz, F. J.; López, J. A.; Meyer, U.; Oro, L. A.; Werner, H. *Inorg. Chem.* **1991**, *30*, 288.

(31) Morse, P. M.; Spencer, M. O.; Wilson, S. R.; Girolami, G. S. *Organometallics* **1994**, *13*, 1646.

in vacuo: yield 88 mg (80%). IR (Nujol):  $\nu(\text{NH})$  3324 cm<sup>-1</sup>,  $\nu(\text{OsH})$  2260, 2171 cm<sup>-1</sup>. <sup>1</sup>H NMR (300 MHz, C<sub>6</sub>D<sub>6</sub>, 293 K):  $\delta$  11.11 (br, 1 H, NH), 8.12 [d,  $J(\text{HH}) = 7.2$  Hz, 1 H, Ph], 7.57 [d,  $J(\text{HH}) = 7.2$  Hz, 2 H, Ph], 7.52 [d,  $J(\text{HH}) = 7.2$  Hz, 1 H, Ph], 7.13 (m, 3 H, Ph), 6.84 (m, 2 H, Ph), 2.43 (m, 6 H, PCH), 1.14 [dvt,  $N = 12.9$  Hz,  $J(\text{HH}) = 6.9$  Hz, 18 H, PCCH<sub>3</sub>], 0.92 [dvt,  $N = 12.9$  Hz,  $J(\text{HH}) = 6.9$  Hz, 18 H, PCCH<sub>3</sub>], -6.78 [t,  $J(\text{PH}) = 12.3$  Hz, 2 H, OsH<sub>2</sub>]. <sup>31</sup>P{<sup>1</sup>H} NMR (121.42 MHz, C<sub>6</sub>D<sub>6</sub>, 293 K):  $\delta$  3.3 (s, t in off-resonance). <sup>13</sup>C{<sup>1</sup>H} NMR (75.42 MHz, C<sub>6</sub>D<sub>6</sub>, 293 K):  $\delta$  176.6 [t,  $J(\text{PC}) = 2.8$  Hz, N=C], 173.9 [t,  $J(\text{PC}) = 4.8$  Hz, Os-C], 145.4, 143.6, 138.1, 130.8, 130.6, 129.4, 129.2, 128.0, 118.8 (all s, Ph), 25.0 [vt,  $N = 24.8$  Hz, PCH], 19.5, 18.9 (both s, PCCH<sub>3</sub>). Anal. Calcd for C<sub>31</sub>H<sub>54</sub>BrNOsP<sub>2</sub>: C, 48.17; H, 7.04; N, 1.81. Found: C, 47.99; H, 6.99; N, 1.77. MS (FAB<sup>+</sup>): *m/e* 771 (M<sup>+</sup> - 2 H). *T*<sub>1</sub> [ms, Os( $\eta^2$ -H<sub>2</sub>), 300 MHz, C<sub>7</sub>D<sub>8</sub>]: 95 (293 K), 72 (273 K), 53 (253 K), 51 (238 K), 50 (233 K), 57, 57 (223 K).

**Preparation of OsBr{NH=C(Ph)C<sub>6</sub>H<sub>4</sub>}( $\eta^2$ -HD)(P<sup>i</sup>Pr<sub>3</sub>)<sub>2</sub> (5-d) and OsBr{NH=C(Ph)C<sub>6</sub>H<sub>4</sub>}( $\eta^2$ -D<sub>2</sub>)(P<sup>i</sup>Pr<sub>3</sub>)<sub>2</sub> (5-d<sub>2</sub>).** This mixture was prepared analogously as described for **4-d** and **4-d<sub>2</sub>**, but using NaBr (5.1 mg, 0.05 mmol). <sup>1</sup>H{<sup>31</sup>P} NMR (300 MHz, CD<sub>2</sub>Cl<sub>2</sub>, 293 K):  $\delta$  -6.99 [td,  $J(\text{HD}) = 6.6$  Hz,  $J(\text{H-NH}) = 3.0$  Hz, OsHD].

**Preparation of OsI{NH=C(Ph)C<sub>6</sub>H<sub>4</sub>}( $\eta^2$ -H<sub>2</sub>)(P<sup>i</sup>Pr<sub>3</sub>)<sub>2</sub> (6).** A solution of **2** (100 mg, 0.14 mmol) in 5 mL of CH<sub>2</sub>Cl<sub>2</sub> was treated with HBF<sub>4</sub> (19.6  $\mu$ L, 0.14 mmol). The resulting red solution obtained was evaporated to dryness, and the residue was treated with a solution of NaI (32.0 mg, 0.14 mmol) in 8 mL of methanol. The red solid obtained was separated by decantation, washed with methanol, and dried in vacuo: yield 94 mg (80%). IR (Nujol):  $\nu(\text{NH})$  3329 cm<sup>-1</sup>,  $\nu(\text{OsH})$  2255, 2164 cm<sup>-1</sup>. <sup>1</sup>H NMR (300 MHz, C<sub>6</sub>D<sub>6</sub>, 293 K):  $\delta$  11.16 (br, 1 H, NH), 8.13 [d,  $J(\text{HH}) = 7.2$  Hz, 1 H, Ph], 7.57 [d,  $J(\text{HH}) = 7.2$  Hz, 2 H, Ph], 7.52 [d,  $J(\text{HH}) = 7.2$  Hz, 1 H, Ph], 7.11 (m, 3 H, Ph), 6.89 [dd,  $J(\text{HH}) = 7.2$  Hz, 1 H, Ph], 6.81 [dd,  $J(\text{HH}) = 7.2$  Hz, 1 H, Ph], 2.50 (m, 6 H, PCH), 1.15 [dvt,  $N = 13.2$  Hz,  $J(\text{HH}) = 6.9$  Hz, 18 H, PCCH<sub>3</sub>], 0.90 [dvt,  $N = 12.3$  Hz,  $J(\text{HH}) = 6.6$  Hz, 18 H, PCCH<sub>3</sub>], -7.72 [t,  $J(\text{PH}) = 12.6$  Hz, 2 H, OsH<sub>2</sub>]. <sup>31</sup>P{<sup>1</sup>H} NMR (121.42 MHz, C<sub>6</sub>D<sub>6</sub>, 293 K):  $\delta$  -2.2 (s, t in off-resonance). <sup>13</sup>C{<sup>1</sup>H} NMR (75.42 MHz, C<sub>6</sub>D<sub>6</sub>, 293 K):  $\delta$  177.9 [d,  $J(\text{PC}) = 2.8$  Hz, N=C], 174.6 [t,  $J(\text{PC}) = 5.1$  Hz, Os-C], 144.7, 142.8, 137.8, 131.1, 130.3, 129.5, 129.2, 119.1 (all s, Ph), 26.4 (vt,  $N = 25.0$  Hz, PCH), 20.0, 19.4 (both s, PCCH<sub>3</sub>). Anal. Calcd for C<sub>31</sub>H<sub>54</sub>INOsP<sub>2</sub>: C, 45.41; H, 6.63; N, 1.70. Found: C, 45.20; H, 6.77; N, 1.64. MS (FAB<sup>+</sup>): *m/e* 819 (M<sup>+</sup> - 2 H). *T*<sub>1</sub> [ms, Os( $\eta^2$ -H<sub>2</sub>), 300 MHz, C<sub>7</sub>D<sub>8</sub>]: 99 (293 K), 75 (273 K), 56 (253 K), 51 (238 K), 50 (233 K), 65, 64 (223 K), 68, 66 (213 K).

**Preparation of OsI{NH=C(Ph)C<sub>6</sub>H<sub>4</sub>}( $\eta^2$ -HD)(P<sup>i</sup>Pr<sub>3</sub>)<sub>2</sub> (6-d) and OsI{NH=C(Ph)C<sub>6</sub>H<sub>4</sub>}( $\eta^2$ -D<sub>2</sub>)(P<sup>i</sup>Pr<sub>3</sub>)<sub>2</sub> (6-d<sub>2</sub>).** This mixture was prepared analogously as described for **4-d** and **4-d<sub>2</sub>**, but using NaI (7.5 mg, 0.05 mmol). <sup>1</sup>H{<sup>31</sup>P} NMR (300 MHz, CD<sub>2</sub>Cl<sub>2</sub>, 293 K):  $\delta$  -7.93 [td,  $J(\text{HD}) = 6.8$  Hz,  $J(\text{H-NH}) = 2.9$  Hz, OsHD].

**X-ray Structure Analysis of OsCl{NH=C(Ph)C<sub>6</sub>H<sub>4</sub>}( $\eta^2$ -H<sub>2</sub>)(P<sup>i</sup>Pr<sub>3</sub>)<sub>2</sub> (4).** Crystals suitable for the X-ray diffraction study were obtained by slow diffusion of methanol into a saturated solution of **4** in dichloromethane. A summary of crystal and refinement data is reported in Table 5. A yellow irregular prism of approximate dimensions 0.57  $\times$  0.55  $\times$  0.44 mm was mounted on a glass fiber at -50 °C. A set of randomly searched reflections in the range  $20 \leq 2\theta \leq 40^\circ$  showed strong reflections, from which a group of 67 were carefully centered and used to obtain by least-squares methods the unit cell dimensions. A Siemens-STOE AED four-circle diffractometer was used for data acquisition ( $\omega/2\theta$  scans), with graphite-monochromated Mo K $\alpha$  radiation and  $2\theta$  range  $3 \leq 2\theta \leq 50^\circ$  ( $-10 \leq h \leq 10$ ,  $-13 \leq l \leq 13$ ,  $-6 \leq k \leq 20$ ). A total of 8170 reflections were measured; 5648 were unique, and 5647 were

**Table 5. Crystal Data and Data Refinement Details for OsCl{NH=C(Ph)C<sub>6</sub>H<sub>4</sub>}( $\eta^2$ -H<sub>2</sub>)(P<sup>i</sup>Pr<sub>3</sub>)<sub>2</sub> (4)**

formula	C <sub>31</sub> H <sub>54</sub> ClNOsP <sub>2</sub>	Z	2
fw	728.34	$\lambda$ , Å	0.71073
space group	P $\bar{1}$ (No. 2)	$\rho$ (calcd), g cm <sup>-3</sup>	1.509
a, Å	8.759(2)	T (K)	223.0(2)
b, Å	11.102(2)	$\mu$ , mm <sup>-1</sup>	4.182
c, Å	17.608(4)	R1 <sup>a</sup>	0.0275
$\alpha$ , deg	74.31(1)	wR2 <sup>b</sup>	0.0745
$\beta$ , deg	76.93(1)	S <sup>c</sup>	0.985
$\gamma$ , deg	83.15(2)		

<sup>a</sup>  $R1(F) = \sum ||F_o| - |F_c|| / \sum |F_o|$ . <sup>b</sup>  $wR2(F^2) = \{ \sum [w(F_o^2 - F_c^2)^2] / \sum [w(F_o^2)^2] \}^{1/2}$ . <sup>c</sup>  $S = \{ \sum [w(F_o^2 - F_c^2)^2] / (n - p) \}^{1/2}$ , where  $n$  is the number of observed reflections and  $p$  is the number of parameters refined.

used in the refinement. Three orientation and intensity standards were monitored every 55 min; no significant variation was observed. Reflections were also corrected for absorption by a semiempirical method ( $\psi$  scans).<sup>32</sup>

The structure was solved by Patterson (osmium atom) and conventional Fourier techniques. Anisotropic thermal parameters were used for all non-hydrogen atoms; hydrogens were included in calculated positions<sup>33</sup> and refined riding on linked atoms with a common isotropic thermal parameter. Hydride ligands were refined as free isotropic atoms with a common isotropic thermal parameter. Final R1( $F$ ,  $F_o > 4.0\sigma(F_o)$ ) and wR2( $F^2$ , all reflections) values were 0.0275 and 0.0745. All calculations were performed by the SHELXTL v. 5.0 system of computer programs.<sup>33</sup>

**Computational Details.** Calculations were performed with the GAUSSIAN 94 series of programs.<sup>34</sup> Geometry optimizations were carried out using density functional theory (DFT)<sup>35</sup> with the B3LYP functional,<sup>36</sup> which has already been used with success to study several dihydrogen and polyhydride systems.<sup>71,37,38</sup>  $C_s$  symmetry has been maintained in the geometry optimizations. A quasirelativistic effective core potential operator was used to represent the 60 innermost electrons of the osmium atom<sup>39a</sup> as well as the electron core of Br and I atoms.<sup>39b</sup> The basis set for the metal atoms was that associated with the pseudopotential,<sup>39a</sup> with a standard double- $\zeta$  LANL2DZ contraction.<sup>34</sup> P and Cl atoms were described with the 6-31G(d) basis set.<sup>40a</sup> The basis set for the hydrogen atoms directly attached to the metal was a double  $\xi$  supplemented with a polarization  $p$  shell.<sup>40b,c</sup> The 6-31G basis set was used for the other H atoms, as well as for carbon and

(32) North, A. C. T.; Phillips, D. C.; Mathews, F. S. *Acta Crystallogr., Sect. A* **1968**, *24*, 351.

(33) Shelldrick, G. M. SHELXTL version 5.0; Siemens Analytical Automation, Inc., Analytical Instrumentation, Madison, WI, 1994.

(34) Frisch, M. J.; Trucks, G. W.; Schlegel, H. B.; Gill, P. M. W.; Johnson, B. G.; Robb, M. A.; Cheeseman, J. R.; Keith, T. A.; Petersson, G. A.; Montgomery, J. A.; Raghavachari, K.; Al-Laham, M. A.; Zakrzewski, V. G.; Ortiz, J. V.; Foresman, J. B.; Ciolowski, J.; Stefanov, B. B.; Nanayakkara, A.; Challacombe, M.; Peng, C. Y.; Ayala, P. Y.; Chen, W.; Wong, M. W.; Andrés, J. L.; Replogle, E. S.; Gomperts, R.; Martin, R. L.; Fox, D. J.; Binkley, J. S.; Defrees, D. J.; Baker, J.; Stewart, J. J. P.; Head-Gordon, M.; González, C.; Pople, J. A. *Gaussian 94*; Gaussian Inc., Pittsburgh, PA, 1995.

(35) (a) Parr, R. G.; Yang, W. *Density Functional Theory of Atoms and Molecules*; Oxford University Press: Oxford, U.K., 1989. (b) Ziegler, T. *Chem. Rev.* **1991**, *91*, 651.

(36) (a) Lee, C.; Yang, W.; Parr, R. G. *Phys. Rev. B* **1988**, *37*, 785. (b) Becke, A. D. *J. Chem. Phys.* **1993**, *98*, 5648. (c) Stephens, P. J.; Devlin, F. J.; Chabalowski, C. F.; Frisch, M. J. *J. Phys. Chem.* **1994**, *98*, 11623.

(37) (a) Maseras, F.; Lledós, A.; Costas, M.; Poblet, J. M. *Organometallics* **1996**, *15*, 2947. (b) Gelabert, R.; Moreno, M.; Lluich, J. M.; Lledós, A. *Organometallics* **1997**, *16*, 3805.

(38) (a) Bacsakay, G. B.; Bytheway, I.; Hush, N. S. *J. Am. Chem. Soc.* **1996**, *118*, 3753. (b) Bytheway, I.; Bacsakay, G. B.; Hush, N. S. *J. Phys. Chem.* **1996**, *100*, 6023.

(39) (a) Hay, P. J.; Wadt, W. R. *J. Chem. Phys.* **1985**, *82*, 299. (b) Wadt, W. R.; Hay, P. J. *J. Chem. Phys.* **1985**, *82*, 284.

nitrogen atoms.<sup>40b</sup> The basis set for the Br and I atoms was that associated with the pseudopotential,<sup>39b</sup> with a standard double- $\zeta$  LANL1DZ contraction,<sup>34</sup> supplemented with a set of d-polarization functions.<sup>40d</sup>

**Acknowledgment.** We acknowledge financial support from the DGES of Spain (Project Nos. PB95-0806

(40) (a) Francl, M. M.; Pietro, W. J.; Hehre, W. J.; Binkley, J. S.; Gordon, M. S.; Defrees, D. J.; Pople, J. A. *J. Chem. Phys.* **1982**, *77*, 3654. (b) Hehre, W. J.; Ditchfield, R.; Pople, J. A. *J. Chem. Phys.* **1972**, *56*, 2257. (c) Hariharan, P. C. Pople, J. A. *Theor. Chim. Acta* **1973**, *28*, 213. (d) Höllwarth, A.; Böhme, M.; Dapprich, S.; Ehlers, A. W.; Gobbi, A.; Jonas, V.; Köhler, K. F.; Stegman, R.; Veldkamp, A.; Frenking, G. *Chem. Phys. Lett.* **1993**, *208*, 237.

and PB95-0639-CO2-01). The use of the computational facilities of the *Centre de Supercomputació i Comunicacions de Catalunya* (C<sup>4</sup>) are gratefully appreciated. Helpful discussions with Prof. J. M. Lluch (UAB, Bellaterra, Spain) are also acknowledged.

**Supporting Information Available:** Tables of atomic coordinates and equivalent isotropic displacement coefficients, anisotropic thermal parameters, experimental details of the X-ray study, bond distances and angles, and interatomic distances for **4** (15 pages). Ordering information is given on any current masthead page.

OM9802820